LASER FUNDAMENTALS

SECOND EDITION

WILLIAM T. SILFVAST
School of Optics / CREOL
University of Central Florida

PUBLISHED BY THE PRESS SYNDICATE OF THE UNIVERSITY OF CAMBRIDGE
The Pitt Building, Trumpington Street, Cambridge, United Kingdom

CAMBRIDGE UNIVERSITY PRESS
The Edinburgh Building, Cambridge CB2 2RU, UK
40 West 20th Street, New York, NY 10011-4211, USA
477 Williamstown Road, Port Melbourne, VIC 3207, Australia
Ruiz de Alarcón 13, 28014 Madrid, Spain
Dock House, The Waterfront, Cape Town 8001, South Africa

http://www.cambridge.org

First published 1996
Reprinted 1999, 2000, 2003

First published 2004

Printed in the United States of America

Typeface Times 10.5/13.5 and Avenir *System* AMS-TEX [FH]

A catalog record for this book is available from the British Library.

Library of Congress Cataloging in Publication data
Silfvast, William Thomas, 1937–
Laser fundamentals / William T. Silfvast. – 2nd ed.
p. cm.
Includes bibliographical references and index.
ISBN 0-521-83345-0
1. Lasers. I. Title.

TA1675.S52 2004
621.36′6 – dc21 2003055352

ISBN 0 521 83345 0 hardback

Contents

Preface to the Second Edition *page* xix
Preface to the First Edition xxi
Acknowledgments xxiii

1 INTRODUCTION 1
OVERVIEW 1
Introduction 1
Definition of the Laser 1
Simplicity of a Laser 2
Unique Properties of a Laser 2
The Laser Spectrum and Wavelengths 3
A Brief History of the Laser 4
Overview of the Book 5

SECTION 1. FUNDAMENTAL WAVE PROPERTIES OF LIGHT

2 WAVE NATURE OF LIGHT – THE INTERACTION OF LIGHT WITH MATERIALS 9
OVERVIEW 9
2.1 Maxwell's Equations 9
2.2 Maxwell's Wave Equations 12
Maxwell's Wave Equations for a Vacuum 12
Solution of the General Wave Equation – Equivalence of Light and Electromagnetic Radiation 13
Wave Velocity – Phase and Group Velocities 17
Generalized Solution of the Wave Equation 20
Transverse Electromagnetic Waves and Polarized Light 21
Flow of Electromagnetic Energy 21
Radiation from a Point Source (Electric Dipole Radiation) 22
2.3 Interaction of Electromagnetic Radiation (Light) with Matter 23
Speed of Light in a Medium 23
Maxwell's Equations in a Medium 24
Application of Maxwell's Equations to Dielectric Materials – Laser Gain Media 25
Complex Index of Refraction – Optical Constants 28
Absorption and Dispersion 29

Estimating Particle Densities of Materials for Use in the Dispersion Equations 34
2.4 Coherence 36
Temporal Coherence 37
Spatial Coherence 38
REFERENCES 39
PROBLEMS 39

SECTION 2. FUNDAMENTAL QUANTUM PROPERTIES OF LIGHT

3 PARTICLE NATURE OF LIGHT – DISCRETE ENERGY LEVELS 45
OVERVIEW 45
3.1 Bohr Theory of the Hydrogen Atom 45
Historical Development of the Concept of Discrete Energy Levels 45
Energy Levels of the Hydrogen Atom 46
Frequency and Wavelength of Emission Lines 49
Ionization Energies and Energy Levels of Ions 51
Photons 54
3.2 Quantum Theory of Atomic Energy Levels 54
Wave Nature of Particles 54
Heisenberg Uncertainty Principle 56
Wave Theory 56
Wave Functions 57
Quantum States 57
The Schrödinger Wave Equation 59
Energy and Wave Function for the Ground State of the Hydrogen Atom 61
Excited States of Hydrogen 63
Allowed Quantum Numbers for Hydrogen Atom Wave Functions 66
3.3 Angular Momentum of Atoms 67
Orbital Angular Momentum 67
Spin Angular Momentum 68
Total Angular Momentum 69
3.4 Energy Levels Associated with One-Electron Atoms 70
Fine Structure of Spectral Lines 70
Pauli Exclusion Principle 72
3.5 Periodic Table of the Elements 72
Quantum Conditions Associated with Multiple Electrons Attached to Nuclei 72
Shorthand Notation for Electronic Configurations of Atoms Having More Than One Electron 76
3.6 Energy Levels of Multi-Electron Atoms 77
Energy-Level Designation for Multi-Electron States 77
Russell–Saunders or *LS* Coupling – Notation for Energy Levels 78
Energy Levels Associated with Two Electrons in Unfilled Shells 79
Rules for Obtaining *S*, *L*, and *J* for *LS* Coupling 82
Degeneracy and Statistical Weights 84
j–j Coupling 85
Isoelectronic Scaling 85

REFERENCES 86
PROBLEMS 86

4 RADIATIVE TRANSITIONS AND EMISSION LINEWIDTH 89
OVERVIEW 89
4.1 Decay of Excited States 90
Radiative Decay of Excited States of Isolated Atoms – Spontaneous Emission 90
Spontaneous Emission Decay Rate – Radiative Transition Probability 94
Lifetime of a Radiating Electron – The Electron as a Classical Radiating Harmonic Oscillator 95
Nonradiative Decay of the Excited States – Collisional Decay 98
4.2 Emission Broadening and Linewidth Due to Radiative Decay 101
Classical Emission Linewidth of a Radiating Electron 101
Natural Emission Linewidth as Deduced by Quantum Mechanics (Minimum Linewidth) 103
4.3 Additional Emission-Broadening Processes 105
Broadening Due to Nonradiative (Collisional) Decay 106
Broadening Due to Dephasing Collisions 107
Amorphous Crystal Broadening 109
Doppler Broadening in Gases 109
Voigt Lineshape Profile 114
Broadening in Gases Due to Isotope Shifts 115
Comparison of Various Types of Emission Broadening 118
4.4 Quantum Mechanical Description of Radiating Atoms 121
Electric Dipole Radiation 122
Electric Dipole Matrix Element 123
Electric Dipole Transition Probability 124
Oscillator Strength 124
Selection Rules for Electric Dipole Transitions Involving Atoms with a Single Electron in an Unfilled Subshell 125
Selection Rules for Radiative Transitions Involving Atoms with More Than One Electron in an Unfilled Subshell 129
Parity Selection Rule 130
Inefficient Radiative Transitions – Electric Quadrupole and Other Higher-Order Transitions 131
REFERENCES 131
PROBLEMS 131

5 ENERGY LEVELS AND RADIATIVE PROPERTIES OF MOLECULES, LIQUIDS, AND SOLIDS 135
OVERVIEW 135
5.1 Molecular Energy Levels and Spectra 135
Energy Levels of Molecules 135
Classification of Simple Molecules 138
Rotational Energy Levels of Linear Molecules 139
Rotational Energy Levels of Symmetric-Top Molecules 141
Selection Rules for Rotational Transitions 141

Vibrational Energy Levels 143
Selection Rule for Vibrational Transitions 143
Rotational–Vibrational Transitions 144
Probabilities of Rotational and Vibrational Transitions 148
Electronic Energy Levels of Molecules 149
Electronic Transitions and Associated Selection Rules of Molecules 150
Emission Linewidth of Molecular Transitions 150
The Franck–Condon Principle 151
Excimer Energy Levels 152
5.2 Liquid Energy Levels and Their Radiation Properties 153
Structure of Dye Molecules 153
Energy Levels of Dye Molecules 155
Excitation and Emission of Dye Molecules 156
Detrimental Triplet States of Dye Molecules 157
5.3 Energy Levels in Solids – Dielectric Laser Materials 158
Host Materials 158
Laser Species – Dopant Ions 159
Narrow-Linewidth Laser Materials 161
Broadband Tunable Laser Materials 166
Broadening Mechanism for Solid-State Lasers 168
5.4 Energy Levels in Solids – Semiconductor Laser Materials 168
Energy Bands in Crystalline Solids 168
Energy Levels in Periodic Structures 170
Energy Levels of Conductors, Insulators, and Semiconductors 172
Excitation and Decay of Excited Energy Levels – Recombination Radiation 173
Direct and Indirect Bandgap Semiconductors 174
Electron Distribution Function and Density of States in Semiconductors 175
Intrinsic Semiconductor Materials 179
Extrinsic Semiconductor Materials – Doping 179
p–n Junctions – Recombination Radiation Due to Electrical Excitation 182
Heterojunction Semiconductor Materials 184
Quantum Wells 186
Variation of Bandgap Energy and Radiation Wavelength with Alloy Composition 191
Recombination Radiation Transition Probability and Linewidth 195
REFERENCES 195
PROBLEMS 195

6 RADIATION AND THERMAL EQUILIBRIUM – ABSORPTION AND STIMULATED EMISSION 199
OVERVIEW 199
6.1 Equilibrium 199
Thermal Equilibrium 199
Thermal Equilibrium via Conduction and Convection 200
Thermal Equilibrium via Radiation 200

6.2 Radiating Bodies 201
Stefan–Boltzmann Law 204
Wien's Law 205
Irradiance and Radiance 206
6.3 Cavity Radiation 207
Counting the Number of Cavity Modes 208
Rayleigh–Jeans Formula 209
Planck's Law for Cavity Radiation 210
Relationship between Cavity Radiation and Blackbody Radiation 211
Wavelength Dependence of Blackbody Emission 214
6.4 Absorption and Stimulated Emission 215
The Principle of Detailed Balance 216
Absorption and Stimulated Emission Coefficients 217
REFERENCES 221
PROBLEMS 221

SECTION 3. LASER AMPLIFIERS

7 CONDITIONS FOR PRODUCING A LASER – POPULATION INVERSIONS, GAIN, AND GAIN SATURATION 225
OVERVIEW 225
7.1 Absorption and Gain 225
Absorption and Gain on a Homogeneously Broadened Radiative Transition (Lorentzian Frequency Distribution) 225
Gain Coefficient and Stimulated Emission Cross Section for Homogeneous Broadening 229
Absorption and Gain on an Inhomogeneously Broadened Radiative Transition (Doppler Broadening with a Gaussian Distribution) 230
Gain Coefficient and Stimulated Emission Cross Section for Doppler Broadening 231
Statistical Weights and the Gain Equation 232
Relationship of Gain Coefficient and Stimulated Emission Cross Section to Absorption Coefficient and Absorption Cross Section 233
7.2 Population Inversion (Necessary Condition for a Laser) 234
7.3 Saturation Intensity (Sufficient Condition for a Laser) 235
7.4 Development and Growth of a Laser Beam 238
Growth of Beam for a Gain Medium with Homogeneous Broadening 238
Shape or Geometry of Amplifying Medium 241
Growth of Beam for Doppler Broadening 244
7.5 Exponential Growth Factor (Gain) 245
7.6 Threshold Requirements for a Laser 247
Laser with No Mirrors 247
Laser with One Mirror 248
Laser with Two Mirrors 249
REFERENCES 253
PROBLEMS 253

8 LASER OSCILLATION ABOVE THRESHOLD 255
OVERVIEW 255
8.1 Laser Gain Saturation 255
Rate Equations of the Laser Levels That Include Stimulated Emission 255
Population Densities of Upper and Lower Laser Levels with Beam Present 256
Small-Signal Gain Coefficient 257
Saturation of the Laser Gain above Threshold 257
8.2 Laser Beam Growth beyond the Saturation Intensity 258
Change from Exponential Growth to Linear Growth 258
Steady-State Laser Intensity 261
8.3 Optimization of Laser Output Power 261
Optimum Output Mirror Transmission 261
Optimum Laser Output Intensity 264
Estimating Optimum Laser Output Power 264
8.4 Energy Exchange between Upper Laser Level Population and Laser Photons 266
Decay Time of a Laser Beam within an Optical Cavity 267
Basic Laser Cavity Rate Equations 268
Steady-State Solutions below Laser Threshold 270
Steady-State Operation above Laser Threshold 272
8.5 Laser Output Fluctuations 273
Laser Spiking 273
Relaxation Oscillations 276
8.6 Laser Amplifiers 279
Basic Amplifier Uses 279
Propagation of a High-Power, Short-Duration Optical Pulse through an Amplifier 280
Saturation Energy Fluence 282
Amplifying Long Laser Pulses 284
Amplifying Short Laser Pulses 284
Comparison of Efficient Laser Amplifiers Based upon Fundamental Saturation Limits 285
Mirror Array and Resonator (Regenerative) Amplifiers 285
REFERENCES 288
PROBLEMS 288

9 REQUIREMENTS FOR OBTAINING POPULATION INVERSIONS 290
OVERVIEW 290
9.1 Inversions and Two-Level Systems 290
9.2 Relative Decay Rates – Radiative versus Collisional 292
9.3 Steady-State Inversions in Three- and Four-Level Systems 293
Three-Level Laser with the Intermediate Level as the Upper Laser Level 295
Three-Level Laser with the Upper Laser Level as the Highest Level 298
Four-Level Laser 301
9.4 Transient Population Inversions 304

9.5 Processes That Inhibit or Destroy Inversions 307
Radiation Trapping in Atoms and Ions 308
Electron Collisional Thermalization of the Laser Levels in Atoms and Ions 311
Comparison of Radiation Trapping and Electron Collisional Mixing in a Gas Laser 315
Absorption within the Gain Medium 316
REFERENCES 319
PROBLEMS 319

10 LASER PUMPING REQUIREMENTS AND TECHNIQUES 322
OVERVIEW 322
10.1 Excitation or Pumping Threshold Requirements 322
10.2 Pumping Pathways 324
Excitation by Direct Pumping 324
Excitation by Indirect Pumping (Pump and Transfer) 327
Specific Pump-and-Transfer Processes 330
10.3 Specific Excitation Parameters Associated with Optical Pumping 339
Pumping Geometries 339
Pumping Requirements 342
A Simplified Optical Pumping Approximation 344
Transverse Pumping 346
End Pumping 348
Diode Pumping of Solid-State Lasers 350
Characterization of a Laser Gain Medium with Optical Pumping (Slope Efficiency) 352
10.4 Specific Excitation Parameters Associated with Particle Pumping 355
Electron Collisional Pumping 355
Heavy Particle Pumping 359
A More Accurate Description of Electron Excitation Rate to a Specific Energy Level in a Gas Discharge 359
Electrical Pumping of Semiconductors 361
REFERENCES 363
PROBLEMS 364

SECTION 4. LASER RESONATORS

11 LASER CAVITY MODES 371
OVERVIEW 371
11.1 Introduction 371
11.2 Longitudinal Laser Cavity Modes 372
Fabry–Perot Resonator 372
Fabry–Perot Cavity Modes 379
Longitudinal Laser Cavity Modes 380
Longitudinal Mode Number 380
Requirements for the Development of Longitudinal Laser Modes 382

11.3 Transverse Laser Cavity Modes 384
Fresnel–Kirchhoff Diffraction Integral Formula 385
Development of Transverse Modes in a Cavity with Plane-Parallel Mirrors 386
Transverse Modes Using Curved Mirrors 390
Transverse Mode Spatial Distributions 391
Transverse Mode Frequencies 392
Gaussian-Shaped Transverse Modes within and beyond the Laser Cavity 393
11.4 Properties of Laser Modes 396
Mode Characteristics 396
Effect of Modes on the Gain Medium Profile 397
REFERENCES 399
PROBLEMS 399
12 STABLE LASER RESONATORS AND GAUSSIAN BEAMS 402
OVERVIEW 402
12.1 Stable Curved Mirror Cavities 402
Curved Mirror Cavities 402
ABCD Matrices 404
Cavity Stability Criteria 406
12.2 Properties of Gaussian Beams 410
Propagation of a Gaussian Beam 411
Gaussian Beam Properties of Two-Mirror Laser Cavities 412
Properties of Specific Two-Mirror Laser Cavities 417
Mode Volume of a Hermite–Gaussian Mode 421
12.3 Properties of Real Laser Beams 423
12.4 Propagation of Gaussian Beams Using *ABCD* Matrices – Complex Beam Parameter 425
Complex Beam Parameter Applied to a Two-Mirror Laser Cavity 428
REFERENCES 432
PROBLEMS 432
13 SPECIAL LASER CAVITIES AND CAVITY EFFECTS 434
OVERVIEW 434
13.1 Unstable Resonators 434
13.2 *Q*-Switching 439
General Description 439
Theory 441
Methods of Producing *Q*-Switching within a Laser Cavity 446
13.3 Gain-Switching 450
13.4 Mode-Locking 451
General Description 451
Theory 451
Techniques for Producing Mode-Locking 456
13.5 Pulse Shortening Techniques 462
Self-Phase Modulation 463
Pulse Shortening or Lengthening Using Group Velocity Dispersion 464
Pulse Compression (Shortening) with Gratings or Prisms 465
Ultrashort-Pulse Laser and Amplifer System 467

13.6 Ring Lasers 468
Monolithic Unidirectional Single-Mode Nd:YAG Ring Laser 469
Two-Mirror Ring Laser 470
13.7 Complex Beam Parameter Analysis Applied to Multi-Mirror Laser Cavities 470
Three-Mirror Ring Laser Cavity 470
Three- or Four-Mirror Focused Cavity 473
13.8 Cavities for Producing Spectral Narrowing of Laser Output 478
Cavity with Additional Fabry–Perot Etalon for Narrow-Frequency Selection 478
Tunable Cavity 478
Broadband Tunable cw Ring Lasers 480
Tunable Cavity for Ultranarrow-Frequency Output 480
Distributed Feedback (DFB) Lasers 481
Distributed Bragg Reflection Lasers 484
13.9 Laser Cavities Requiring Small-Diameter Gain Regions – Astigmatically Compensated Cavities 484
13.10 Waveguide Cavities for Gas Lasers 485
REFERENCES 486
PROBLEMS 488

SECTION 5. SPECIFIC LASER SYSTEMS

14 LASER SYSTEMS INVOLVING LOW-DENSITY GAIN MEDIA 491
OVERVIEW 491
14.1 Atomic Gas Lasers 491
Introduction 491
Helium–Neon Laser 492
General Description 492
Laser Structure 493
Excitation Mechanism 494
Applications 497
Argon Ion Laser 497
General Description 497
Laser Structure 498
Excitation Mechanism 499
Krypton Ion Laser 500
Applications 501
Helium–Cadmium Laser 501
General Description 501
Laser Structure 502
Excitation Mechanism 504
Applications 505
Copper Vapor Laser 505
General Description 505
Laser Structure 507
Excitation Mechanism 507
Applications 509

14.2 Molecular Gas Lasers 510
Introduction 510
Carbon Dioxide Laser 511
General Description 511
Laser Structure 511
Excitation Mechanism 515
Applications 515
Excimer Lasers 516
General Description 516
Laser Structure 517
Excitation Mechanism 518
Applications 520
Nitrogen Laser 520
General Description 520
Laser Structure and Excitation Mechanism 521
Applications 522
Far-Infrared Gas Lasers 522
General Description 522
Laser Structure 523
Excitation Mechanism 523
Applications 524
Chemical Lasers 524
General Description 524
Laser Structure 524
Excitation Mechanism 524
Applications 525
14.3 X-Ray Plasma Lasers 525
Introduction 525
Pumping Energy Requirements 525
Excitation Mechanism 528
Optical Cavities 532
X-Ray Laser Transitions 532
Applications 532
14.4 Free-Electron Lasers 535
Introduction 535
Laser Structure 536
Applications 537
REFERENCES 537

15 LASER SYSTEMS INVOLVING HIGH-DENSITY GAIN MEDIA 539
OVERVIEW 539
15.1 Organic Dye Lasers 539
Introduction 539
Laser Structure 540
Excitation Mechanism 543
Applications 544
15.2 Solid-State Lasers 545
Introduction 545

Ruby Laser 547
General Description 547
Laser Structure 548
Excitation Mechanism 548
Applications 549
Neodymium YAG and Glass Lasers 550
General Description 550
Laser Structure 551
Excitation Mechanism 553
Applications 554
Neodymium:YLF Lasers 555
General Description 555
Laser Structure 556
Excitation Mechanism 556
Applications 557
Neodymium:Yttrium Vanadate ($Nd:YVO_4$) Lasers 557
General Description 557
Laser Structure 557
Excitation Mechanism 558
Applications 558
Ytterbium:YAG Lasers 559
General Description 559
Laser Structure 560
Excitation Mechanism 560
Applications 561
Alexandrite Laser 562
General Description 562
Laser Structure 563
Excitation Mechanism 563
Applications 564
Titanium Sapphire Laser 565
General Description 565
Laser Structure 566
Excitation Mechanism 567
Applications 568
Chromium LiSAF and LiCAF Lasers 568
General Description 568
Laser Structure 568
Excitation Mechanism 569
Applications 570
Fiber Lasers 570
General Description 570
Laser Structure 571
Excitation Mechanism 571
Applications 572
Color Center Lasers 573
General Description 573
Laser Structure 574

Excitation Mechanism 574
Applications 576
15.3 Semiconductor Diode Lasers 576
Introduction 576
Four Basic Types of Laser Materials 579
Laser Structure 581
Frequency Control of Laser Output 591
Quantum Cascade Lasers 592
p-Doped Germanium Lasers 594
Excitation Mechanism 594
Applications 596
REFERENCES 597

SECTION 6. FREQUENCY MULTIPLICATION OF LASER BEAMS

16 FREQUENCY MULTIPLICATION OF LASERS AND OTHER NONLINEAR OPTICAL EFFECTS 601
OVERVIEW 601
16.1 Wave Propagation in an Anisotropic Crystal 601
16.2 Polarization Response of Materials to Light 603
16.3 Second-Order Nonlinear Optical Processes 604
Second Harmonic Generation 604
Sum and Difference Frequency Generation 605
Optical Parametric Oscillation 607
16.4 Third-Order Nonlinear Optical Processes 607
Third Harmonic Generation 608
Intensity-Dependent Refractive Index – Self-Focusing 609
16.5 Nonlinear Optical Materials 610
16.6 Phase Matching 610
Description of Phase Matching 610
Achieving Phase Matching 613
Types of Phase Matching 615
16.7 Saturable Absorption 615
16.8 Two-Photon Absorption 617
16.9 Stimulated Raman Scattering 618
16.10 Harmonic Generation in Gases 619
REFERENCES 619

Appendix 621
Index 625

1
Introduction

OVERVIEW A laser is a device that amplifies light and produces a highly directional, high-intensity beam that most often has a very pure frequency or wavelength. It comes in sizes ranging from approximately one tenth the diameter of a human hair to the size of a very large building, in powers ranging from 10^{-9} to 10^{20} W, and in wavelengths ranging from the microwave to the soft–X-ray spectral regions with corresponding frequencies from 10^{11} to 10^{17} Hz. Lasers have pulse energies as high as 10^{4} J and pulse durations as short as 5×10^{-15} s. They can easily drill holes in the most durable of materials and can weld detached retinas within the human eye. They are a key component of some of our most modern communication systems and are the "phonograph needle" of our compact disc players. They perform heat treatment of high-strength materials, such as the pistons of our automobile engines, and provide a special surgical knife for many types of medical procedures. They act as target designators for military weapons and provide for the rapid check-out we have come to expect at the supermarket. What a remarkable range of characteristics for a device that is in only its fifth decade of existence!

INTRODUCTION

There is nothing magical about a laser. It can be thought of as just another type of light source. It certainly has many unique properties that make it a special light source, but these properties can be understood without knowledge of sophisticated mathematical techniques or complex ideas. It is the objective of this text to explain the operation of the laser in a simple, logical approach that builds from one concept to the next as the chapters evolve. The concepts, as they are developed, will be applied to all classes of laser materials, so that the reader will develop a sense of the broad field of lasers while still acquiring the capability to study, design, or simply understand a specific type of laser system in detail.

DEFINITION OF THE LASER

The word *laser* is an acronym for Light Amplification by Stimulated Emission of Radiation. The laser makes use of processes that increase or amplify light signals after those signals have been generated by other means. These processes include (1) stimulated emission, a natural effect that was deduced by considerations relating to thermodynamic equilibrium, and (2) optical feedback (present in most

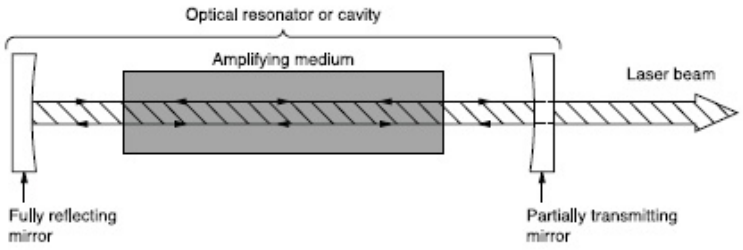

Figure 1-1 Simplified schematic of typical laser

lasers) that is usually provided by mirrors. Thus, in its simplest form, a laser consists of a gain or amplifying medium (where stimulated emission occurs), and a set of mirrors to feed the light back into the amplifier for continued growth of the developing beam, as seen in Figure 1-1.

SIMPLICITY OF A LASER

The simplicity of a laser can be understood by considering the light from a candle. Normally, a burning candle radiates light in all directions, and therefore illuminates various objects equally if they are equidistant from the candle. A laser takes light that would normally be emitted in all directions, such as from a candle, and concentrates that light into a single direction. Thus, if the light radiating in all directions from a candle were concentrated into a single beam of the diameter of the pupil of your eye (approximately 3 mm), and if you were standing a distance of 1 m from the candle, then the light intensity would be 1,000,000 times as bright as the light that you normally see radiating from the candle! That is essentially the underlying concept of the operation of a laser. However, a candle is not the kind of medium that produces amplification, and thus there are no candle lasers. It takes relatively special conditions within the laser medium for amplification to occur, but it is that capability of taking light that would normally radiate from a source in all directions – and concentrating that light into a beam traveling in a single direction – that is involved in making a laser. These special conditions, and the media within which they are produced, will be described in some detail in this book.

UNIQUE PROPERTIES OF A LASER

The beam of light generated by a typical laser can have many properties that are unique. When comparing laser properties to those of other light sources, it can be readily recognized that the values of various parameters for laser light either greatly exceed or are much more restrictive than the values for many common light sources. We never use lasers for street illumination, or for illumination within our houses. We don't use them for searchlights or flashlights or as headlights in

our cars. Lasers generally have a narrower frequency distribution, or much higher intensity, or a much greater degree of collimation, or much shorter pulse duration, than that available from more common types of light sources. Therefore, we do use them in compact disc players, in supermarket check-out scanners, in surveying instruments, and in medical applications as a surgical knife or for welding detached retinas. We also use them in communications systems and in radar and military targeting applications, as well as many other areas. *A laser is a specialized light source that should be used only when its unique properties are required.*

THE LASER SPECTRUM AND WAVELENGTHS

A portion of the electromagnetic radiation spectrum is shown in Figure 1-2 for the region covered by currently existing lasers. Such lasers span the wavelength range from the far infrared part of the spectrum ($\lambda = 1{,}000\ \mu$m) to the soft–X-ray region ($\lambda = 3$ nm), thereby covering a range of wavelengths of almost six orders of magnitude. There are several types of units that are used to define laser wavelengths. These range from micrometers or microns (μm) in the infrared to nanometers (nm) and angstroms (Å) in the visible, ultraviolet (UV), vacuum ultraviolet (VUV), extreme ultraviolet (EUV or XUV), and soft–X-ray (SXR) spectral regions.

WAVELENGTH UNITS

$1\ \mu\text{m} = 10^{-6}$ m;
$1\ \text{Å} = 10^{-10}$ m;
$1\ \text{nm} = 10^{-9}$ m.

Consequently, 1 micron (μm) = 10,000 angstroms (Å) = 1,000 nanometers (nm). For example, green light has a wavelength of 5×10^{-7} m = 0.5 μm = 5,000 Å = 500 nm.

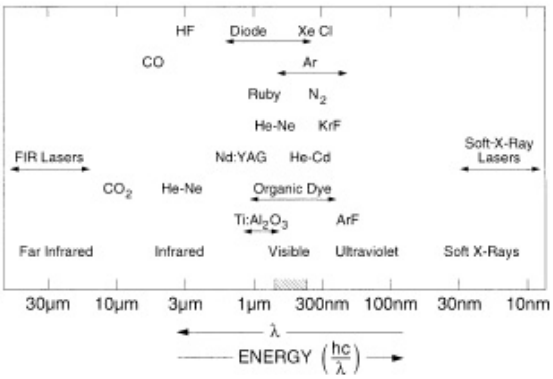

Figure 1-2 Wavelength range of various lasers

WAVELENGTH REGIONS

Far infrared: 10 to 1,000 μm;
middle infrared: 1 to 10 μm;
near infrared: 0.7 to 1 μm;
visible: 0.4 to 0.7 μm, or 400 to 700 nm;
ultraviolet: 0.2 to 0.4 μm, or 200 to 400 nm;
vacuum ultraviolet: 0.1 to 0.2 μm, or 100 to 200 nm;
extreme ultraviolet: 10 to 100 nm;
soft X-rays: 1 nm to approximately 20–30 nm (some overlap with EUV).

A BRIEF HISTORY OF THE LASER

Charles Townes took advantage of the stimulated emission process to construct a microwave amplifier, referred to as a *maser*. This device produced a coherent beam of microwaves to be used for communications. The first maser was produced in ammonia vapor with the inversion between two energy levels that produced gain at a wavelength of 1.25 cm. The wavelengths produced in the maser were comparable to the dimensions of the device, so extrapolation to the optical regime – where wavelengths were five orders of magnitude smaller – was not an obvious extension of that work.

In 1958, Townes and Schawlow published a paper concerning their ideas about extending the maser concept to optical frequencies. They developed the concept of an optical amplifier surrounded by an optical mirror resonant cavity to allow for growth of the beam. Townes and Schawlow each received a Nobel Prize for his work in this field.

In 1960, Theodore Maiman of Hughes Research Laboratories produced the first laser using a ruby crystal as the amplifier and a flashlamp as the energy source. The helical flashlamp surrounded a rod-shaped ruby crystal, and the optical cavity was formed by coating the flattened ends of the ruby rod with a highly reflecting material. An intense red beam was observed to emerge from the end of the rod when the flashlamp was fired!

The first gas laser was developed in 1961 by A. Javan, W. Bennett, and D. Harriott of Bell Laboratories, using a mixture of helium and neon gases. At the same laboratories, L. F. Johnson and K. Nassau demonstrated the first neodymium laser, which has since become one of the most reliable lasers available. This was followed in 1962 by the first semiconductor laser, demonstrated by R. Hall at the General Electric Research Laboratories. In 1963, C. K. N. Patel of Bell Laboratories discovered the infrared carbon dioxide laser, which is one of the most efficient and powerful lasers available today. Later that same year, E. Bell of Spectra Physics discovered the first ion laser, in mercury vapor. In 1964 W. Bridges of Hughes Research Laboratories discovered the argon ion laser, and in 1966 W. Silfvast, G. R. Fowles, and B. D. Hopkins produced the first blue helium–cadmium metal vapor

laser. During that same year, P. P. Sorokin and J. R. Lankard of the IBM Research Laboratories developed the first liquid laser using an organic dye dissolved in a solvent, thereby leading to the category of broadly tunable lasers. Also at that time, W. Walter and co-workers at TRG reported the first copper vapor laser.

The first vacuum ultraviolet laser was reported to occur in molecular hydrogen by R. Hodgson of IBM and independently by R. Waynant et al. of the Naval Research Laboratories in 1970. The first of the well-known rare-gas–halide excimer lasers was observed in xenon fluoride by J. J. Ewing and C. Brau of the Avco–Everett Research Laboratory in 1975. In that same year, the first quantum-well laser was made in a gallium arsenide semiconductor by J. van der Ziel and co-workers at Bell Laboratories. In 1976, J. M. J. Madey and co-workers at Stanford University demonstrated the first free-electron laser amplifier operating in the infrared at the CO_2 laser wavelength. In 1979, Walling and co-workers at Allied Chemical Corporation obtained broadly tunable laser output from a solid-state laser material called alexandrite, and in 1985 the first soft–X-ray laser was successfully demonstrated in a highly ionized selenium plasma by D. Matthews and a large number of co-workers at the Lawrence Livermore Laboratories. In 1986, P. Moulton discovered the titanium sapphire laser. In 1991, M. Hasse and co-workers developed the first blue-green diode laser in ZnSe. In 1994, F. Capasso and co-workers developed the quantum cascade laser. In 1996, S. Nakamura developed the first blue diode laser in GaN-based materials.

In 1961, Fox and Li described the existence of resonant transverse modes in a laser cavity. That same year, Boyd and Gordon obtained solutions of the wave equation for confocal resonator modes. Unstable resonators were demonstrated in 1969 by Krupke and Sooy and were described theoretically by Siegman. *Q*-switching was first obtained by McClung and Hellwarth in 1962 and described later by Wagner and Lengyel. The first mode-locking was obtained by Hargrove, Fork, and Pollack in 1964. Since then, many special cavity arrangements, feedback schemes, and other devices have been developed to improve the control, operation, and reliability of lasers.

OVERVIEW OF THE BOOK

Isaac Newton described light as small bodies emitted from shining substances. This view was no doubt influenced by the fact that light appears to propagate in a straight line. Christian Huygens, on the other hand, described light as a wave motion in which a small source spreads out in all directions; most observed effects – including diffraction, reflection, and refraction – can be attributed to the expansion of primary waves and of secondary wavelets. The dual nature of light is still a useful concept, whereby the choice of particle or wave explanation depends upon the effect to be considered.

Section One of this book deals with the fundamental *wave* properties of light, including Maxwell's equations, the interaction of electromagnetic radiation with

matter, absorption and dispersion, and coherence. Section Two deals with the fundamental *quantum* properties of light. Chapter 3 describes the concept of discrete energy levels in atomic laser species and also how the periodic table of the elements evolved. Chapter 4 deals with radiative transitions and emission linewidths and the probability of making transitions between energy levels. Chapter 5 considers energy levels of lasers in molecules, liquids, and solids – both dielectric solids and semiconductors. Chapter 6 then considers radiation in equilibrium and the concepts of absorption and stimulated emission of radiation. At this point the student has the basic tools to begin building a laser.

Section Three considers laser amplifiers. Chapter 7 describes the theoretical basis for producing population inversions and gain. Chapter 8 examines laser gain and operation above threshold, Chapter 9 describes how population inversions are produced, and Chapter 10 considers how sufficient amplification is achieved to make an intense laser beam. Section Four deals with laser resonators. Chapter 11 considers both longitudinal and transverse modes within a laser cavity, and Chapter 12 investigates the properties of stable resonators and Gaussian beams. Chapter 13 considers a variety of special laser cavities and effects, including unstable resonators, Q-switching, mode-locking, pulse narrowing, ring lasers, and spectral narrowing.

Section Five covers specific laser systems. Chapter 14 describes eleven of the most well-known gas and plasma laser systems. Chapter 15 considers twelve well-known dye lasers and solid-state lasers, including both dielectric solid-state lasers and semiconductor lasers. The book concludes with Section Six (Chapter 16), which provides a brief overview of frequency muliplication with lasers and other nonlinear effects.

6

Radiation and Thermal Equilibrium

Absorption and Stimulated Emission

OVERVIEW Chapters 3 through 5 dealt with energy levels of gaseous, liquid, and solid materials and discussed the spontaneous radiative properties associated with transitions occurring between those levels. The rate of radiation occurring from energy levels was described in terms of transition probabilities and relative oscillator strengths of the transitions. So far, no attempt has been made to consider the collective properties of a large number of radiating atoms or molecules. Such considerations will be dealt with in this chapter and will lead to the concept of radiation in thermodynamic equilibrium. Planck's radiation law evolved from the analysis of equilibrium radiation from dense bodies. From this law and other principles, Einstein was able to deduce the concept of stimulated emission, which is the underlying principle leading to the development of the laser.

6.1 EQUILIBRIUM

Thermal Equilibrium

We will consider the processes that bring various masses into equilibrium when they are located near each other. In the study of thermodynamics, *thermal equilibrium* describes the case where all of the individual masses within a closed system have the same temperature. If a substance of small mass M1 and temperature T1 is placed near to or in contact with a much larger mass M2 at a higher temperature T2, then the state of thermal equilibrium is achieved when the mass M1 reaches the same temperature as that of M2. The duration over which this occurs could be a period as short as picoseconds or as long as minutes or even hours, depending upon the situation. In fact, the final temperature will be less than T2, since M2 will also be cooled slightly as it transfers some of its energy to M1. The temperature decrease of M2 will depend upon the relative masses of M1 and M2, but the relevant factor, when a new equilibrium is reached, is that the total energy will be divided equally among all of the atoms of the combined system. Thermal equilibrium can be achieved between the two masses by one or more possible heat transfer processes: conduction, convection, and radiation.

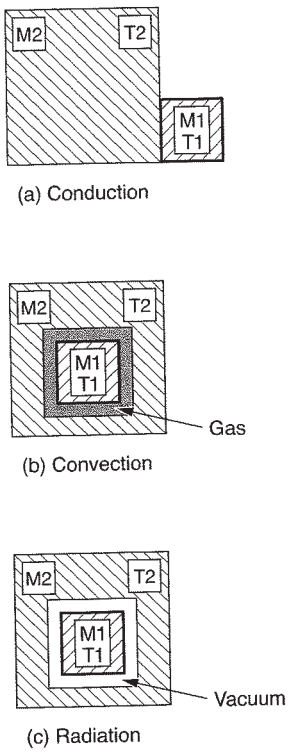

Figure 6-1 Examples of energy transfer via (a) conduction, (b) convection, and (c) radiation

Thermal Equilibrium via Conduction and Convection

If M1 is placed in direct contact with M2, as shown in Figure 6-1(a), this will generally bring the masses to equilibrium in the shortest period of time. In this case, the method of heat transfer is referred to as *conduction*. If M1 and M2 are composed of two metals, for example, the rapid heat transfer by the conduction electrons of the metals would bring the two masses quickly to an equilibrium temperature.

If the bodies are placed as shown in Figure 6-1(b), with M1 located in a large cavity inside M2, and if a gas (such as air) at atmospheric pressure fills the cavity between M1 and M2, then the molecules of the gas would provide the energy transport from M2 to M1 and so bring M1 and M2 to a final equilibrium temperature somewhere between T1 and T2. This case of energy transport leading to thermal equilibrium is referred to as *convection*. A small portion of the energy would also end up in the gas, which would arrive at the same final equilibrium temperature as that of the two masses. Since the mass density of gas at atmospheric pressure is approximately three orders of magnitude lower than that of solids, the convection process takes a much longer time to reach equilibrium than does the conduction process.

Thermal Equilibrium via Radiation

If all of the air is evacuated from the space between M1 and M2 as in Figure 6-1(c), so that there is no material contact between them, there is still another process that

will bring the two masses into equilibrium – namely, *radiation*. For such a process to occur, two effects must take place: the masses must be radiating energy, and they must be capable of absorbing radiation from the other body.

6.2 RADIATING BODIES

We will first consider the question of whether or not the masses are radiating. If a collection of atoms is at temperature T then, according to the Boltzmann equation, the probability distribution function f_i that any atom has a discrete energy E_i is given by

$$f_i(E_i) = C_1 g_i e^{-E_i/kT}. \tag{6.1}$$

In this equation, Boltzmann's constant k is 8.6164×10^{-5} eV/K and g_i is the statistical weight of level i. The C_1 term is a normalizing constant that is the same for all energy levels and is subject to the constraint that

$$\sum_i f_i = \sum_i C_1 g_i e^{-E_i/kT} = 1, \tag{6.2}$$

which suggests that the electron must exist in one of the i energy levels. If N is the total number of atoms per unit volume of this species and N_i is the population density occupying a specific energy level i, then

$$\sum_i N_i = N, \tag{6.3}$$

where N_i could then be expressed as

$$N_i = f_i N = C_1 g_i e^{-E_i/kT} N. \tag{6.4}$$

For a high-density material such as a solid, the energy levels are usually continuously distributed (with some exceptions, including insulators such as solid-state laser host materials and their dopant ions). Thus the distribution function would be expressed as a probability per unit energy $g(E)$ such that the probability of finding a fraction of that material excited to a specific energy E within an energy width dE would be given by

$$g(E)\,dE = C_2 e^{-E/kT}\,dE, \tag{6.5}$$

where we have ignored the statistical weights. This probability would also be subject to the normalizing constraint that

$$\int_0^\infty g(E)\,dE = \int_0^\infty C_2 e^{-E/kT}\,dE = 1. \tag{6.6}$$

From this equation we can readily show that $C_2 = 1/kT$, and thus $g(E)$ can be expressed as

$$g(E) = \frac{1}{kT} e^{-E/kT}. \tag{6.7}$$

Again, if N is the total number of atoms per unit volume in the solid and if we refer to the number of atoms per unit volume within a specific energy range dE as $N(E)$, then the normalizing condition requires that

$$N = \int_0^\infty N(E)\,dE. \tag{6.8}$$

The number of atoms at energy E within a specific energy range dE can thus be given as

$$N(E)\,dE = \frac{N}{kT} e^{-E/kT}\,dE. \tag{6.9}$$

We can compute the ratio of the populations that exists at two specific energies, either for the case of discrete energy levels such as those for isolated atoms or for high-density materials such as solids. For discrete energy levels, according to (6.4) the ratio of the population densities N_u and N_l (number of particles per unit volume) of atoms with electrons occupying energy levels u and l (with corresponding energies E_u and E_l) would be expressed as

$$\frac{N_u}{N_l} = \frac{g_u}{g_l} e^{-(E_u - E_l)/kT} = \frac{g_u}{g_l} e^{-\Delta E_{ul}/kT}, \tag{6.10}$$

where it is assumed that E_u is higher than E_l and that $\Delta E_{ul} = E_u - E_l$. Similarly, the ratio of population densities of a dense material (such as a solid) at energies E_u and E_l within an energy interval dE can be expressed from (6.9) as

$$\frac{N(E_u)\,dE}{N(E_l)\,dE} = \frac{N(E_u)}{N(E_l)} = e^{-\Delta E_{ul}/kT}. \tag{6.11}$$

In dense materials there are so many sublevels within small ranges of energy that the statistical weights for most levels are essentially the same; hence they would effectively cancel in an expression such as (6.11). It can thus be seen that (6.10) and (6.11) are identical except for the statistical weight factor, which we have ignored for the high-density material. Therefore, when a collection of atoms – whether in the form of a gas, a liquid, or a solid – are assembled together and reach equilibrium, not only the kinetic energies related to their motion will be in thermal equilibrium; the distribution of their internal energies associated with the specific energy levels they occupy will also be in thermal equilibrium, according to (6.10) and (6.11).

EXAMPLE

Determine the temperature required to excite electrons of atoms within a solid to energies sufficient to produce radiation in the visible portion of the electromagnetic spectrum when the electrons decay from those excited levels.

We assume a typical solid material with a density of approximately $N = 5 \times 10^{28}$ atoms/m^3 in the ground state. For several different temperatures we will

compute how many of those atoms would occupy energy levels high enough to radiate that energy as visible light. Visible radiation comprises wavelengths ranging from 700 nm in the red to 400 nm in the violet, or photons with energies ranging from approximately 1.7 to 3.1 eV. We would thus be interested in energy levels above 1.7 eV that are populated within the solid, since any electron having an energy higher than 1.7 eV will have the potential of radiating a visible photon. We will calculate the number of species that have an electron in an excited energy level that lies higher than 1.7 eV above the ground state for several different temperatures by taking the integral of $N(E)\,dE$ from (6.9) over the energy range from 1.7 eV to infinity. We must recognize that, for a typical solid, most of the atoms will decay nonradiatively from these excited levels, but a certain portion could emit visible radiation depending upon the radiation efficiency of the material.

At room temperature, $T \cong 300$ K and $kT = 0.026$ eV. Thus N_{vis} can be expressed as

$$N_{\text{vis}} \cong \frac{N}{kT}\int_{1.7\text{ eV}}^{\infty} e^{-E/kT}\,dE = -N[e^{-E/kT}]_{1.7\text{ eV}}^{\infty}$$
$$= (-5\times 10^{28})[0 - 4\times 10^{-29}] \cong \frac{0}{\text{m}^3}. \tag{6.12}$$

Thus there are essentially no atoms in this energy range from which visible photons could radiate. This is, of course, why we can see nothing when we enter a room that has no illumination, even though the human eye is very sensitive and can detect as little as only a few photons. No thermal radiation in the visible spectrum could be emitted from the walls, floors, ceiling, or furniture when those various masses are at room temperature.

We next consider a temperature of 1,000 K or 0.086 eV. At this temperature we determine the population able to emit visible photons as

$$N_{\text{vis}} = \frac{N}{kT}\int_{1.7\text{ eV}}^{\infty} e^{-E/kT}\,dE = -N[e^{-E/kT}]_{1.7\text{ eV}}^{\infty}$$
$$= (-5\times 10^{28})[0 - 2.6\times 10^{-9}] = \frac{1.3\times 10^{20}}{\text{m}^3}. \tag{6.13}$$

Thus, increasing the temperature by little more than a factor of 3, we have gone from essentially no atoms in those excited levels to an appreciable number in those levels. We can and do see such radiation: in the glowing coals of a campfire, in the glowing briquettes of a barbecue fire, or from the heating elements of an electric stove; all are at temperatures of approximately 1,000 K.

A temperature of 5,000 K or 0.43 eV (the temperature of the sun) can also be considered for comparison:

$$N_{\text{vis}} = \frac{N}{kT}\int_{1.7\text{ eV}}^{\infty} e^{-E/kT}\,dE = -N[e^{-E/kT}]_{1.7\text{ eV}}^{\infty}$$
$$= (-5\times 10^{28})[0 - 1.9\times 10^{-2}] = \frac{9.5\times 10^{26}}{\text{m}^3}. \tag{6.14}$$

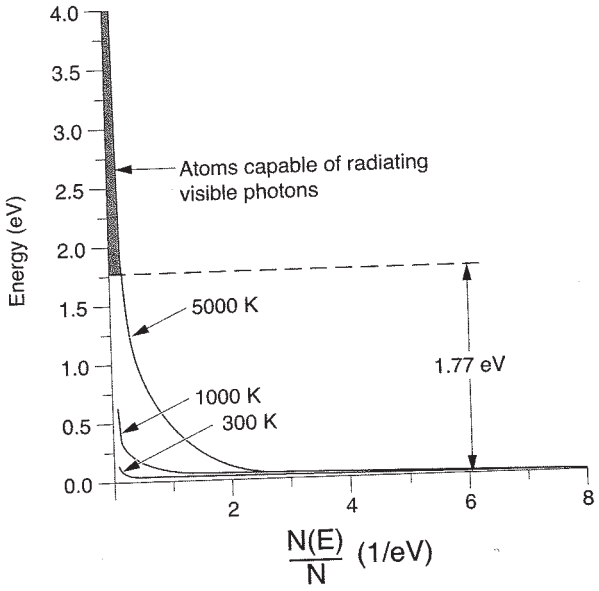

Figure 6-2 Population distribution of occupied states versus energy for temperatures of 300 K, 1,000 K, and 5,000 K

At this temperature nearly 10% of the atoms would be excited to an energy of 1.7 eV or higher, and the material would be radiating with an intensity that is too bright to look at.

A graph of $N(E)/N$, which is the distribution of population versus energy as taken from (6.9), is plotted in Figure 6-2 for 300 K, 1,000 K, and 5,000 K. The graph clearly shows the rapid increase in the population at higher energies as the temperature is increased. It can be seen that the energy levels that are high enough to produce visible radiation are populated only when the temperature is significantly above room temperature, as discussed in the preceding examples. Such radiation emitted from masses at those various temperatures would emit a continuous spectrum of frequencies over a certain frequency range. The radiation is referred to as *thermal radiation,* since it is emitted from objects in thermal equilibrium.

There are two effects we should consider when observing thermal radiation such as that of glowing coals. First, more energy is radiated from the object as the temperature is increased; this is described by the Stefan–Boltzmann law. Second, if the spectral content of the radiation from the glowing coals is analyzed, it will be found that the radiation increases with decreasing wavelength to a maximum value at a specific wavelength, and then it decreases relatively rapidly at even shorter wavelengths. The wavelength at which the maximum value occurs can be obtained from Wien's law.

Stefan–Boltzmann Law

The Stefan–Boltzmann law is an empirical relationship obtained by Stefan and later derived theoretically by Boltzmann. It states that the total radiated intensity

(W/m^2) emitted from a body at temperature T is proportional to the fourth power of the temperature, T^4. This can be written as

$$I = e_M \sigma T^4, \tag{6.15}$$

where $\sigma = 5.67 \times 10^{-8}$ W/m^2-K^4 and e_M is the emissivity that is specific for a given material. The emissivity, a dimensionless quantity that varies between zero and unity, represents the ability of a body to radiate efficiently and is also associated with its ability to absorb radiation, as will be discussed in more detail in Section 6.3. Equation (6.15) describes an extremely rapidly increasing function with temperature and accounts for the tremendous flux increase we estimated to be radiating in the visible from our simple system at 300 K, 1,000 K, and 5,000 K. The total radiation from such a mass would increase in going from 300 K to 1,000 K by a factor of 123, and in going from 300 K to 5,000 K by a factor of over 77,000!

Wien's Law

A graph of the spectrum of radiation emitted versus frequency from a heated mass is shown for three different temperatures in Figure 6-3. The specific wavelength at which the radiation is a maximum was found to vary inversely with temperature. The wavelength λ_m at which the maximum emission occurs for any given temperature is described by Wien's law as follows:

$$\lambda_m T = 2.898 \times 10^{-3} \text{ m-K}. \tag{6.16}$$

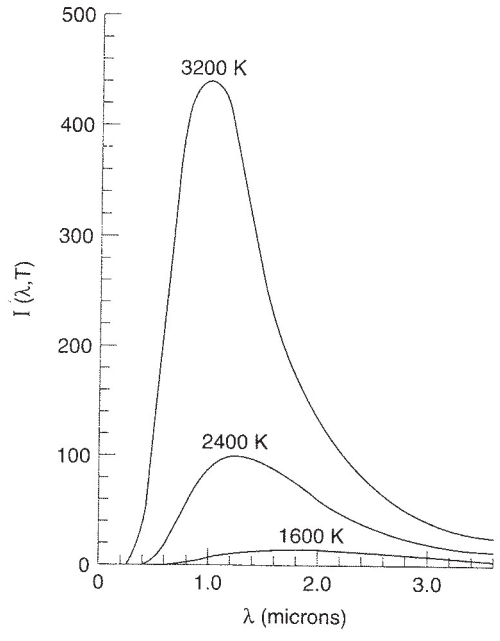

Figure 6-3 Spectrum of radiation versus wavelength of a heated mass (blackbody) for several temperatures

TABLE 6-1
Total Emissivity e_M at Low Temperatures

Highly polished silver	0.02
Aluminum	0.08
Copper	0.15
Cast iron	0.25
Polished brass	0.60
Black gloss paint	0.90
Lampblack	0.95

Irradiance and Radiance

Recall the case depicted in Figure 6-1(c). Because M2 is initially at a higher temperature than M1, we surmise that M1 will eventually be raised to equilibrium with M2, at a temperature T3 such that T1 < T3 < T2, by absorbing the radiation from M2. However, when M1 reaches the same temperature as M2, *it must radiate as much energy as it absorbs.* Otherwise, it would continue to heat up to a higher temperature than T2, which defies the laws of thermodynamics. Thus the relationship – in total power per unit area – between the *irradiance* I_1 incident upon M1 and the *radiance* H_1 leaving M1 must be proportional:

$$H_1 = b_1 I_1 \quad \text{or} \quad I_1 = \frac{H_1}{b_1}, \tag{6.17}$$

where $b_1 \leq 1$ is the proportionality constant that represents the fraction of the power absorbed by M1. If instead of just M1 there were several masses (M1, M3, and M4) all inside the cavity of M2, we could express their radiative characteristics with respect to the incident flux in the same way as that of (6.17) for M1. We would obtain the relationships $H_1 = b_1 I_1$, $H_3 = b_3 I_3$, and $H_4 = b_4 I_4$. Because I (the power per unit area) arriving at each body would be the same, we can write

$$I = \frac{H_1}{b_1} = \frac{H_3}{b_3} = \frac{H_4}{b_4} = \cdots, \tag{6.18}$$

which indicates that the ratio of the power radiated from a body to the fraction of radiation absorbed is a constant, independent of the material. Thus strong absorbers are also strong radiators, and since b represents the fraction of radiation absorbed we can conclude that $b = e_M$. This relationship is known as *Kirchhoff's law.* Examples of emissivity are shown in Table 6-1. It can be seen that emissivities range from very small numbers for highly reflecting materials to values near unity for highly absorbing materials. Lampblack, the soot deposited from burning candles, is perhaps the blackest material we ever observe; it has an emissivity of $e_M = 0.95$.

The ideal case of a perfect absorber ($b = \varepsilon_M = 1$) is also a perfect emitter in that it would radiate as much energy as is incident upon it. Such a perfectly absorbing body is known as a blackbody (since it appears to be very black in color)

and is the best emitter of thermal radiation. The radiation it emits is consequently referred to as blackbody radiation. If such a blackbody is placed within a cavity in thermal equilibrium – say, M1 in Figure 6-1(c) – then it would radiate an intensity and frequency distribution that is characteristic of the thermal radiation within the medium because the radiance would be equal to the thermal radiation (irradiance) within the cavity. Hence blackbody radiation is also referred to as cavity radiation.

6.3 CAVITY RADIATION

We have developed the idea that ideal blackbodies radiate with the same spectral power as that occurring within a cavity in thermal equilibrium such as the radiation within the cavity depicted in Figure 6-1(c). It will be useful for us to obtain the quantity and wavelength distribution of the radiated flux within such a cavity in order to later obtain the stimulated emission coefficient, which is the fundamental concept leading to amplification in a laser medium. We must allow for the possibility of all frequencies of radiation within the cavity and would like to obtain an expression describing that frequency distribution for any specific temperature. Toward this end, we begin by considering the properties of radiation within a cavity. The boundary conditions – as deduced from electromagnetic theory – suggest that, in order for electromagnetic waves to be supported or enhanced (or at least not rapidly die away), the value of the electric vector must be zero at the boundary of the cavity. This involves the development of distinct "standing waves" within the cavity – that is, waves whose functions exhibit no time dependence. Such standing waves, which have a value of zero for the electric field at the boundaries, are referred to as *cavity modes.* The existence of each mode implies that the wave has an integral number of half-wavelengths occurring along the wave direction within the cavity. For example, three distinct cavity modes oriented in a specific direction are shown in Figure 6-4: waves of one half-wavelength, two half-wavelengths (one complete cycle), and three half-wavelengths. If we can calculate the number of such modes at each frequency or wavelength within a cavity and multiply by the average energy of each mode at those wavelengths, we can obtain the frequency

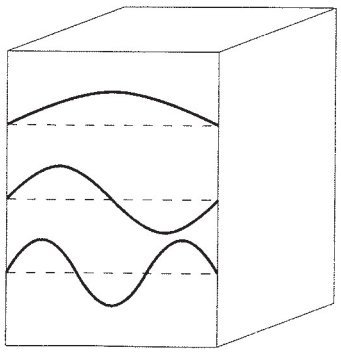

Figure 6-4 Several modes of electromagnetic radiation within a confined cavity

distribution of the emission spectrum for cavity radiation. Hence we will now calculate the number of modes that exist within a cavity of a given size.

Counting the Number of Cavity Modes

We will carry out a counting procedure for these modes in a way similar to that used in Section 5.4 for counting the number of modes available for electrons in the conduction band of a semiconductor. Assume we have a cavity that is rectangular in shape with dimensions L_x, L_y, and L_z, as shown in Figure 6-1(c). Because we are considering only standing waves within the cavity, in counting the number of modes we will include only the spatial dependence of the electromagnetic waves, which is described by an oscillatory function of the form $e^{-i(k_xL_x+k_yL_y+k_zL_z)}$. In order to satisfy the boundary condition that the field be periodic in L and also zero at the boundaries, the exponential phase factor must be an integral multiple of π. This can be achieved if we specify individual modes in the directions x, y, z such that

$$k_xL_x = n_x\pi, \quad k_yL_y = n_y\pi, \quad k_zL_z = n_z\pi, \qquad n_x, n_y, n_z = 0, 1, 2, \ldots. \tag{6.19}$$

Any mode in this cavity will have a specific value of k; its mode number can be identified by specifying mode numbers n_x, n_y, n_z since

$$k^2 = (k_x^2 + k_y^2 + k_z^2) = \left[\left(\frac{n_x\pi}{L_x}\right)^2 + \left(\frac{n_y\pi}{L_y}\right)^2 + \left(\frac{n_z\pi}{L_z}\right)^2\right]. \tag{6.20}$$

The total number of modes in any volume $V = L_xL_yL_z$ up to a given value of k can then be counted by using a three-dimensional space whose axes are defined as the number of modes. For example, the number of modes in the x direction would be the length of the cavity in that direction L_x divided by one half-wavelength or $n_x = L_x/(\lambda/2)$, which is equivalent to the mode number in that direction. Consequently, the number of modes along each axis of the volume for a specific wavelength λ is obtained as $n_x = 2L_x/\lambda$, $n_y = 2L_y/\lambda$, and $n_z = 2L_z/\lambda$. We will choose one octant of an ellipsoid to describe the mode volume, since this is a convenient way of counting the modes. (We choose only one octant with the foregoing dimensions for the major axes because all of the values of n are positive.) Each mode – say $n_x = 1$, $n_y = 2$, and $n_z = 1$, for example – is specified in our mode volume as the intersection of those specific mode numbers within that octant, as shown in Figure 6-5. Such a mode can be specified, for the purposes of this calculation, by assuming that it is represented by a cube of unit dimensions within that volume. This approximation is very good for volumes that are significantly larger than the wavelength λ, and since we are dealing with relatively small (short) wavelengths, the volume calculation for counting the number of modes is quite accurate.

The volume of the octant can be written as

$$\frac{1}{8}\cdot\frac{4\pi}{3}\cdot n_xn_yn_z = \frac{1}{8}\cdot\frac{4\pi}{3}\left(\frac{2L_x}{\lambda}\cdot\frac{2L_y}{\lambda}\cdot\frac{2L_z}{\lambda}\right); \tag{6.21}$$

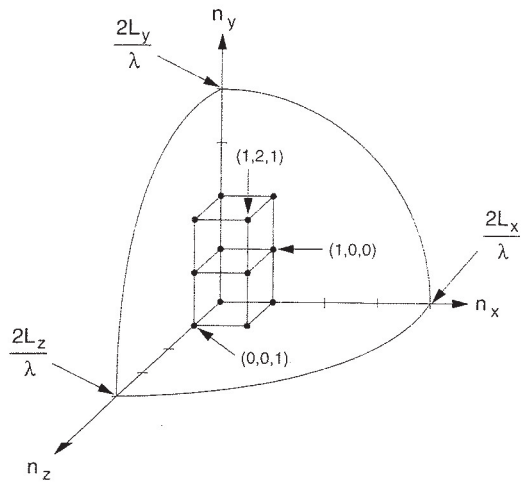

Figure 6-5
Three-dimensional diagram of the cavity mode volume

likewise, the number of modes M can be expressed as

$$M = \frac{1}{8} \cdot \frac{4\pi}{3}\left(\frac{2L_x 2L_y 2L_z}{\lambda^3}\right) = \frac{4\pi\eta^3\nu^3}{3c^3}V, \tag{6.22}$$

where $V = L_x L_y L_z$ and we have used the relationship $\lambda\nu = c/\eta$. This calculation defines the number of modes for *all frequencies up to and including the frequency* ν within a volume V. This number must be doubled to allow for the fact that two orthogonal polarizations of the electromagnetic waves must be represented for each spatial mode. Higher frequencies would be outside of this volume and thus would not be counted. For frequencies up to the value ν, the mode density ρ (number of modes per unit volume) is then given by

$$\rho(\nu) = \frac{2M}{V} = \frac{8\pi\eta^3\nu^3}{3c^3}. \tag{6.23}$$

This equation can be differentiated to obtain the number of modes per unit volume within a given frequency interval between ν and $\nu + d\nu$,

$$\frac{d\rho(\nu)}{d\nu} = \frac{8\pi\eta^3\nu^2}{c^3}. \tag{6.24}$$

We have used a rectangular cavity to derive the mode density as well as the mode density per unit frequency for the number of modes up to frequency ν, but it can be shown that (6.23) and (6.24) are generally applicable formulas for any shape of cavity.

Rayleigh–Jeans Formula

If we assume that the average energy per mode is of the order of kT, then we can obtain the Rayleigh–Jeans formula for the energy density $u(\nu)$ of radiation per unit

volume within the frequency ν to $\nu + d\nu$. We do this by multiplying the mode density per unit frequency by the average energy kT per mode. Therefore, using kT as the value of the energy per mode, for the energy density per unit frequency we have

$$u(\nu) = \frac{d\rho(\nu)}{d\nu} kT = \frac{8\pi\eta^3\nu^2}{c^3} kT. \tag{6.25}$$

This result suggests that there is a continuous increase in energy density with frequency for a given temperature T. This expression is referred to as the Rayleigh–Jeans formula for the energy density of cavity radiation. It agrees with experiments for lower frequencies but does not predict the experimentally observed maximum value for a given temperature at higher frequencies as shown in Figure 6.3. Instead, the Rayleigh–Jeans expression suggests that energy density approaches infinity as the frequency is increased.

Planck's Law for Cavity Radiation

Planck was disturbed by the invalidity of the Rayleigh–Jeans formula for the intensity of cavity radiation at higher frequencies and so he questioned the basic assumption of assigning a value of kT for the average energy per cavity mode. As an alternative, Planck explored the possibility of quantizing the mode energy, postulating that an oscillator of frequency ν could have only discrete values $mh\nu$ of energy, where $m = 0, 1, 2, 3, \ldots$. He referred to this unit of energy $h\nu$ as a quantum that could not be further divided. We can apply this condition to obtain the energy of each cavity mode in thermal equilibrium. We will use the Boltzmann distribution function (eqn. 6.1) to describe the energy distribution of the modes; however, we will assign discrete values for the energy $E_m = mh\nu$ in the function instead of a continuous variable E, and we will ignore the statistical weight factor since we are talking about very dense materials. Thus, for a given temperature T, we can express the distribution function as

$$f_m = Ce^{-E_m/kT} = Ce^{-mh\nu/kT}. \tag{6.26}$$

The normalizing condition for the distribution function requires that

$$\sum_{m=0}^{\infty} f_m = \sum_{m=0}^{\infty} Ce^{-mh\nu/kT} = C\sum_{m=0}^{\infty} e^{-mh\nu/kT} = 1, \tag{6.27}$$

which can be solved for C to obtain

$$C = 1 - e^{-h\nu/kT}. \tag{6.28}$$

We can then compute the average mode energy $\bar{E}$ of those oscillators in the usual manner:

$$\bar{E} = \frac{\sum_{m=0}^{\infty} E_m f_m}{\sum_{m=0}^{\infty} f_m} = \frac{C\sum_{m=0}^{\infty}(mh\nu)e^{-mh\nu/kT}}{C\sum_{m=0}^{\infty} e^{-mh\nu/kT}}$$
$$= \frac{[1-e^{-h\nu/kT}]\sum_{m=0}^{\infty}(mh\nu)e^{-mh\nu/kT}}{1}. \tag{6.29}$$

The value of the summation in the numerator on the right-hand side of (6.29) is

$$\sum_{m=0}^{\infty}(mh\nu)e^{-mh\nu/kT} = h\nu\sum_{m=0}^{\infty} me^{-mh\nu/kT} = \frac{h\nu e^{-h\nu/kT}}{(1-e^{-h\nu/kT})^2}. \tag{6.30}$$

This leads to an expression for the average energy $\bar{E}$ of

$$\bar{E} = \frac{h\nu}{e^{h\nu/kT}-1}. \tag{6.31}$$

Using this expression for the average energy per mode instead of the kT value used in the Rayleigh–Jeans law to obtain (6.25), we arrive at the following relationship for the energy density per unit frequency:

$$u(\nu) = \frac{8\pi h\eta^3\nu^3}{c^3(e^{h\nu/kT}-1)}. \tag{6.32}$$

This relationship has a maximum at a specific frequency for a given temperature, and both the location of the maximum and the shape of the distribution agree very well with experimental observations. This expression became known as Planck's law for cavity radiation.

The expression $u(\nu)$ describes the energy density per unit frequency ν for radiation anywhere within an enclosed cavity in thermal equilibrium at temperature T. It consists of waves traveling in all directions within the cavity. If we wanted to compute the total energy density u emitted at all frequencies, we could of course simply integrate the energy density $u(\nu)\,d\nu$ over the frequencies:

$$u = \int_0^{\infty} u(\nu)\,d\nu. \tag{6.33}$$

Carrying out this integration leads to the Stefan–Boltzmann law.

Relationship between Cavity Radiation and Blackbody Radiation

If we were able to make a small hole of unit area through mass M2 into the cavity within M2 of Figure 6-1(c), we would observe a small amount of radiation of intensity $I(\nu)$ at any specific frequency ν emerging from the hole; that intensity is related to the energy density $u(\nu)$ within the cavity. We could then calculate the total radiation flux emerging from that cavity at frequency ν, through the hole,

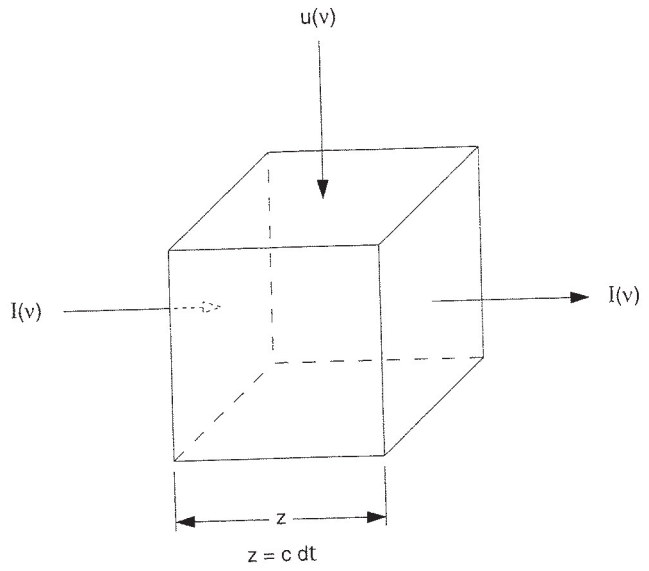

Figure 6-6 Beam of light intensity $I(\nu)$ incident upon a volume of thickness $z = c\,dt$

traveling in all directions within a solid angle of 2π (a hemisphere). This value for the radiation flux at frequency ν would describe the irradiance of a blackbody, since we deduced earlier that the spectral density within a cavity has the same energy density as that at the surface of a blackbody. We will therefore refer to this radiation as the blackbody radiation intensity per unit frequency, or $I_{BB}(\nu)$.

Before performing this calculation, we need to obtain a relationship between the energy density $u(\nu)$ (energy per unit volume-frequency) of electromagnetic radiation within a volume element and the flux $I(\nu)$ (energy per time-area-frequency) passing through a surface enclosing part of that volume element and traveling in a specific direction, as shown in Figure 6-6. Let us consider a beam of light of intensity per unit frequency $I(\nu)$ at frequency ν, with a cross-sectional area dA and traveling in a direction z that passes through that area dA in a time dt. The energy density of radiation would be the product of the intensity of the beam, the cross-sectional area, and the time duration, or $I(\nu)\,dA\,dt$, which has units of energy per unit frequency. This would be equivalent to considering the energy density $u(\nu)$ of a beam existing within a volume $dV = dA \cdot z$ if an instantaneous photograph were taken of the beam within that volume dV of length $z = v\,dt$, where v is the velocity of the beam. This is described by the expression

$$I(\nu)\,dA\,dt = u(\nu)\,dV = u(\nu)\,dA \cdot z = u(\nu)\,dA \cdot v\,dt. \tag{6.34}$$

If the volume element is in a vacuum then $v \equiv c$, which leads to the relationship

$$I(\nu) = u(\nu)c \tag{6.35}$$

for a beam traveling in *a specific direction*.

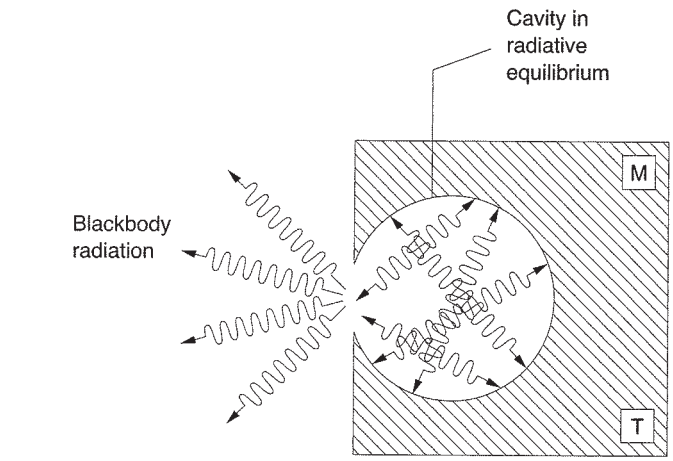

Figure 6-7(a) Blackbody radiation escaping from a cavity within mass *M* at equilibrium temperature *T*

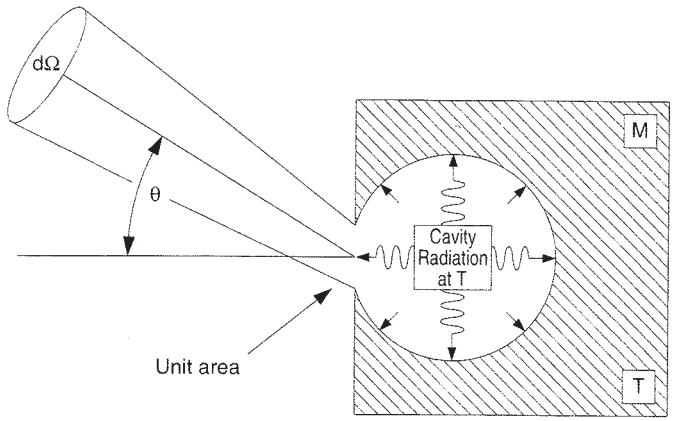

Figure 6-7(b) Coordinates for analyzing blackbody radiation escaping from a confined cavity

When the volume element is in a medium whose index of refraction is η, the velocity is expressed as $v = c/\eta$; this leads to

$$I(\nu) = u(\nu)\frac{c}{\eta}. \tag{6.36}$$

We can now convert the expression for the energy density of radiation within a cavity of temperature T to an expression for blackbody radiation emerging from a hole of unit surface area accessing that cavity and radiating into a hemisphere, as indicated in Figure 6-7(a). Radiation from any point within the cavity is traveling in all directions – that is, within a 4π solid angle. We consider the coordinates shown in Figure 6-7(b), where the fraction of radiation traveling within a solid angle $d\Omega/4\pi$ at a particular angle θ with respect to the normal to the plane of the hole is described by $I(\nu)\cos\theta\, d\Omega/4\pi$. In this expression we have assumed that the intensity emitted from the source is independent of angle, but the factor $\cos\theta$ represents the decrease in the effective area of the hole with increasing angle from the normal as seen by the observer. Expressing the solid angle as $d\Omega = \sin\theta\, d\theta\, d\phi$,

the radiation flux in that direction can be written as $I(\nu)\cos\theta\sin\theta\,d\theta\,d\phi/4\pi$. The total blackbody flux $I_{BB}(\nu)$ is obtained by integrating this component of the flux over the entire hemisphere (2π solid angle):

$$I_{BB}(\nu) = \int_0^{2\pi}\int_0^{\pi/2} \frac{I(\nu)\cos\theta\sin\theta\,d\theta\,d\phi}{4\pi}. \tag{6.37}$$

Replacing $I(\nu)$ by $u(\nu)c$ from (6.35) gives the relationship between the blackbody radiation intensity per unit frequency, $I_{BB}(\nu)$, and the energy density per unit frequency, $u(\nu)$, of the cavity:

$$I_{BB}(\nu) = \int_0^{2\pi}\int_0^{\pi/2} u(\nu)c\cdot\frac{\cos\theta\sin\theta\,d\theta\,d\phi}{4\pi} = \frac{u(\nu)c}{4}. \tag{6.38}$$

Using (6.38) in conjunction with the value of $u(\nu)$ indicated in (6.32), we can obtain the spectral radiance of a blackbody as a function of ν and T as follows:

$$I_{BB}(\nu) = \frac{2\pi h\nu^3}{c^2}\frac{1}{e^{h\nu/kT}-1}. \tag{6.39}$$

Wavelength Dependence of Blackbody Emission

The total radiance of $I_{BB}(\nu)$ from a frequency interval $d\nu$ is given as

$$I_{BB}(\nu)\,d\nu = \frac{2\pi h\nu^3}{c^2}\frac{d\nu}{e^{h\nu/kT}-1}. \tag{6.40}$$

Because $\lambda\nu = c$ (i.e., $\nu = c/\lambda$), it follows that

$$|d\nu| = \frac{c}{\lambda^2}\,d\lambda. \tag{6.41}$$

We can therefore express the intensity per unit wavelength at temperature T as

$$I_{BB}(\lambda, T) = \frac{2\pi c^2 h}{\lambda^5(e^{ch/\lambda kT}-1)}. \tag{6.42}$$

The total radiance emitted from the blackbody surface within a specific wavelength interval $\Delta\lambda$ would then be expressed as

$$I_{BB}(\lambda, \Delta\lambda, T) = I_{BB}(\lambda, T)\Delta\lambda. \tag{6.43}$$

Specific values of the radiance $I_{BB}(\lambda, \Delta\lambda, T)$ as given by (6.43), in units of power per unit area (intensity) over the wavelength interval $\Delta\lambda$, can be obtained from the following empirical expression for $I_{BB}(\lambda, T)$:

$$I_{BB}(\lambda, T) = \frac{3.75 \times 10^{-22}}{\lambda^5(e^{0.0144/\lambda T} - 1)} \text{ W/m}^2\text{-}\mu\text{m}, \tag{6.44}$$

where λ must be given in meters, $\Delta\lambda$ in micrometers (μm), and T in degrees Kelvin. Alternatively,

$$I_{BB}(\lambda, T) = \frac{3.75 \times 10^{-25}}{\lambda^5(e^{0.0144/\lambda T} - 1)} \text{ W/m}^2\text{-nm} \tag{6.45}$$

for λ in meters, $\Delta\lambda$ in nanometers, and T in degrees Kelvin. Remember that these expressions are for the radiation into a 2π steradian solid angle.

EXAMPLE

Compute the radiation flux or power in watts coming from a surface of temperature 300 K (near room temperature) and area 0.02 m^2 over a wavelength interval of 0.1 μm at a wavelength of 1.0 μm.

Use (6.43) and (6.44) to obtain the intensity (W/m^2) and multiply it by the area ΔA (m^2) to obtain the power P in watts coming from the surface:

$$\begin{aligned} P &= I_{BB}(\lambda, T)\Delta\lambda\Delta A \\ &= \frac{3.75 \times 10^{-22}}{(1 \times 10^{-6})^5(e^{0.0144/(1\times10^{-6})300} - 1)}(0.1)(0.02) = 1.06 \times 10^{-15} \text{ W}. \end{aligned}$$

We can see that at room temperature the power radiated from a blackbody within this wavelength region is almost too small to be measurable.

6.4 ABSORPTION AND STIMULATED EMISSION

We have examined the issues relating to the decay of electrons from a higher energy level to a lower level. We have also investigated the natural radiative decay process, which is inherent in all excited states of all materials and is referred to as *spontaneous emission*. However, we saw in Chapter 4 that such emission is not always the dominant decay process. We described how collisions with other particles (in the case of gases) or phonons (in the case of solids) can depopulate a level faster than the normal radiative process. Such collisions can also populate or *excite* energy levels.

Excitation or de-excitation can also occur by way of photons – "light particles" that have specific energies. The phenomenon of light producing excitation, referred to as *absorption*, has been known for well over 100 years. Such a process

could also have been referred to as "stimulated" absorption, since it requires electromagnetic energy to stimulate the electron and thereby produce the excitation. There is no reason to suppose that the inverse of that process would not also occur, but it was never seriously considered until Einstein suggested the concept of stimulated emission in 1917.

The Principle of Detailed Balance

Einstein was considering the recently developed Planck law for cavity radiation, the expression we just derived. He began questioning how the principle of detailed balance must apply in the case of radiation in equilibrium, a situation associated with cavity radiation. This principle states that, *in equilibrium,* the total number of particles leaving a certain quantum state per unit time equals the number arriving in that state per unit time. It also states that in equilibrium the number leaving by a particular pathway equals the number arriving by that pathway.

We tacitly used this principle in the first part of this chapter when arguing that the mass M1 could not continue to receive excess energy from M2 once it had reached the new equilibrium temperature. The principle describes why the population of a specific energy state cannot increase indefinitely. This principle has also been called the principle of *microscopic reversibility* and was originally applied to considerations of thermodynamic equilibrium.

The principle of detailed balance suggests that if a photon can stimulate an electron to move from a lower energy state l to higher energy state u by means of absorption, then a photon should also be able to stimulate an electron from the same upper state u to the lower state l. In the case of absorption, the photon disappears, with the energy being transferred to the absorbing species. In the case of stimulation, or stimulated emission, the species would have to radiate an additional photon to conserve energy. Such a stimulated emission process must occur in order to keep the population of the two energy levels in thermal equilibrium, if that equilibrium is determined by cavity radiation as described earlier in this chapter. Thus, the relationships between absorption and stimulated emission must be associated in some way with the Planck law for radiation in thermal equilibrium.

We have identified the three radiative processes producing interactions between two bound levels in a material: spontaneous emission, absorption (stimulated absorption), and stimulated emission. These processes are diagrammed in Figure 6-8. In the case of both of the stimulated processes (absorption and stimulated emission) occurring between bound (discrete) states, the energy (related to the frequency) of the light must correspond exactly to that of the energy difference between the two energy states. For stimulated emission, an additional photon is emitted at exactly the same energy (or frequency) as that of the incident photon (conservation of energy), and in exactly the same direction in phase with the incident photon (conservation of momentum).

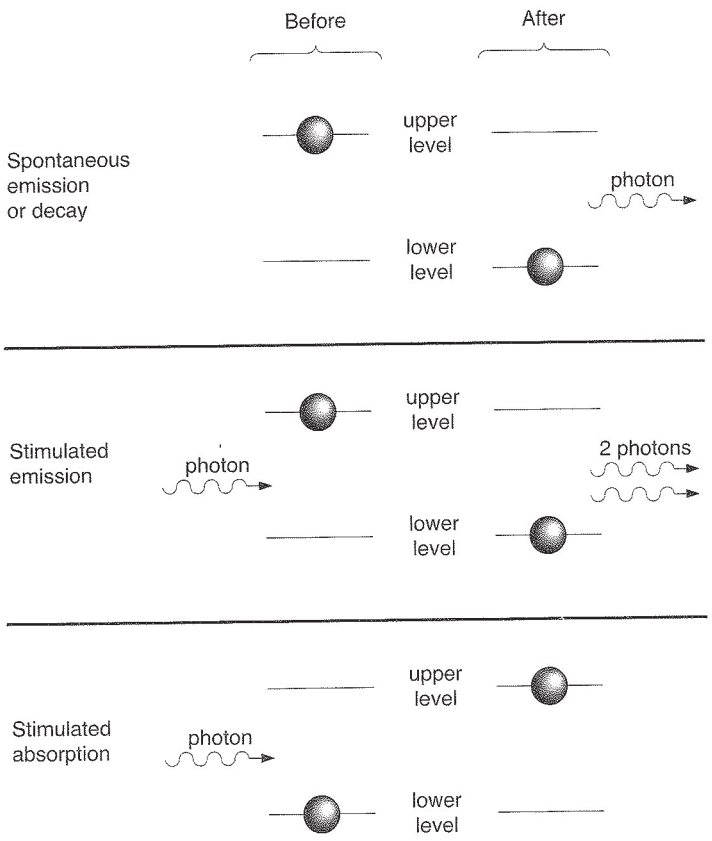

Figure 6-8 The three fundamental radiation processes associated with the interaction of light with matter: spontaneous emission, stimulated emission, and absorption

Absorption and Stimulated Emission Coefficients

We will now derive the absorption and stimulated emission coefficients associated with these processes by considering radiation in thermal equilibrium. We will consider a group of atoms having electrons occupying either energy levels u or l with population densities N_u and N_l (number of atoms per unit volume). We assume the atoms are in thermal equilibrium with each other and must therefore be related by the Boltzmann distribution function given in (6.10),

$$\frac{N_u}{N_l} = \frac{g_u}{g_l} e^{-(E_u - E_l)/kT} = \frac{g_u}{g_l} e^{-\Delta E_{ul}/kT}, \tag{6.46}$$

where g_u and g_l are the statistical weights of levels u and l and where $E_u - E_l = \Delta E_{ul}$.

We will consider photons interacting with such a collection of atoms. The photons will be assumed to have energies ΔE_{ul} such that $\Delta E_{ul} = h\nu_{ul}$, corresponding to the exact difference in energy between the levels u and l. We have defined A_{ul} as the spontaneous transition probability, the rate at which spontaneous transitions

occur from level u to level l (number per unit time). Thus, the number of spontaneous transitions from u to l per unit time per unit volume is simply $N_u A_{ul}$.

We have also suggested that stimulated processes should occur. These processes would be proportional to the photon energy density $u(\nu)$ at frequency ν_{ul} as well as to the population in the appropriate level. If we assume that the proportionality constant for such stimulated transitions is B, then the upward flux – the number of stimulated upward transitions per unit volume per unit time per unit frequency – would be $N_l B_{lu} u(\nu)$. Similarly, the downward flux would be $N_u B_{ul} u(\nu)$. The constants A_{ul}, B_{ul}, and B_{lu} are referred to as the Einstein A and B coefficients.

For the populations N_u and N_l to be in *radiative thermal equilibrium* (as described by eqn. 6.46) and for the principle of detailed balance to apply, the downward radiative flux should equal the upward radiative flux between the two levels:

$$N_u A_{ul} + N_u B_{ul} u(\nu) = N_l B_{lu} u(\nu). \tag{6.47}$$

From this equation we can solve for $u(\nu)$ as follows:

$$u(\nu) = \frac{N_u A_{ul}}{N_l B_{lu} - N_u B_{ul}}. \tag{6.48}$$

Dividing the top and bottom terms in the right-hand side of (6.48) by N_u and then using (6.46) for the ratio N_u/N_l, we are led to the expression

$$u(\nu) = \frac{A_{ul}}{B_{ul}} \left(\left[\frac{g_l B_{lu}}{g_u B_{ul}} \right] e^{h\nu_{ul}/kT} - 1 \right)^{-1}, \tag{6.49}$$

where we have used the relationship $\Delta E_{ul} = h\nu_{ul}$.

Equation (6.49) has a familiar form if we compare it to (6.32). Since both equations concern radiation in thermal equilibrium, if true then they must be equivalent. The equivalence follows if

$$\frac{g_l B_{lu}}{g_u B_{ul}} = 1 \quad \text{or} \quad g_l B_{lu} = g_u B_{ul} \tag{6.50}$$

and

$$\frac{A_{ul}}{B_{ul}} = \frac{8\pi h \eta^3 \nu^3}{c^3}. \tag{6.51}$$

We have thus derived the relationship between the stimulated emission and absorption coefficients B_{ul} and B_{lu} (respectively), along with their relationship to the spontaneous emission coefficient A_{ul}. We can rewrite (6.51) to obtain

$$B_{ul} = \frac{c^3}{8\pi h \eta^3 \nu^3} A_{ul}. \tag{6.52}$$

We can now substitute the expression for A_{ul} in terms of $A_{ul}(\nu)$ from (4.64) to obtain

$$B_{ul} = \frac{c^3}{8\pi h\eta^3\nu^3} \frac{(\nu - \nu_0)^2 + (\gamma_{ul}^T/4\pi)^2}{\gamma_{ul}^T/4\pi^2} A_{ul}(\nu). \tag{6.53}$$

If we now define

$$B_{ul}(\nu) = \frac{\gamma_{ul}^T/4\pi^2}{(\nu - \nu_0)^2 + (\gamma_{ul}^T/4\pi)^2} B_{ul}, \tag{6.54}$$

which describes the frequency dependence of B_{ul}, then (6.53) may be rewritten as

$$\frac{A_{ul}(\nu)}{B_{ul}(\nu)} = \frac{8\pi h\eta^3\nu^3}{c^3} \equiv \frac{A_{ul}}{B_{ul}}. \tag{6.55}$$

Hence the frequency-dependent expressions for $B_{ul}(\nu)$ and $B_{lu}(\nu)$ will satisfy (6.49) if

$$\frac{g_l B_{lu}(\nu)}{g_u B_{ul}(\nu)} = 1 \quad \text{or} \quad g_l B_{lu}(\nu) = g_u B_{ul}(\nu). \tag{6.56}$$

We have thus derived the stimulated emission coefficients B_{ul} and B_{lu}, as well as their frequency-dependent counterparts $B_{ul}(\nu)$ and $B_{lu}(\nu)$, that define the way a photon beam interacts with a two-level system of atoms that was obtained by considering radiation in thermal equilibrium. These relationships provide the fundamental concepts necessary for producing a laser.

It is interesting to examine the ratio of stimulated to spontaneous emission rates from level u. This ratio can be obtained from (6.32) and (6.51) as

$$\frac{B_{ul}u(\nu)}{A_{ul}} = \frac{1}{e^{h\nu_{ul}/kT} - 1}. \tag{6.57}$$

Thus, stimulated emission plays a significant role only for temperatures in which kT is of, or greater than, the order of the photon energy $h\nu_{ul}$. The ratio is unity when $h\nu_{ul}/kT = \ln 2 = 0.693$. For visible transitions in the green portion of the spectrum (photons of the order of 2.5 eV), such a relationship would be achieved for a temperature of 33,500 K. Thus, in the visible spectrum, the dominance of stimulated emission over spontaneous emission normally happens only in stars, in high-temperature and -density laboratory plasmas such as laser-produced plasmas, or in lasers. In low-pressure plasmas the radiation can readily escape, so there is no opportunity for the radiation density to build up to a value where the stimulated decay rate is comparable to the radiative decay rate. In lasers, however, the ratio of (6.57) can be significantly greater than unity.

EXAMPLE

A helium–neon laser operating at 632.8 nm has an output power of 1.0 mW with a 1-mm beam diameter. The beam passes through a mirror that has 99% reflectivity and 1% transmission at the laser wavelength. What is the ratio of $B_{ul}u(\nu)/A_{ul}$

for this laser? What is the effective blackbody temperature of the laser beam as it emerges from the laser output mirror? Assume the beam diameter is also 1 mm inside the laser cavity and that the power is uniform over the beam cross section (this is only an approximation, as we will learn in Chapter 11). Assume also that the laser linewidth is approximately one tenth of the Doppler width for the transition.

The laser frequency is determined by

$$\nu = \frac{c}{\lambda} = \frac{3 \times 10^8 \text{ m/s}}{6.328 \times 10^{-7} \text{ m}} = 4.74 \times 10^{14} \text{ Hz}.$$

From (6.51) we can now compute the ratio of A_{ul}/B_{ul} for $\eta = 1$ as

$$\frac{A_{ul}}{B_{ul}} = \frac{8\pi h\nu^3}{c^3} = \frac{(8\pi)(6.63 \times 10^{-34} \text{ J-s})(4.74 \times 10^{14} \text{ Hz})^3}{(3 \times 10^8 \text{ m/s})^3}$$
$$= 6.57 \times 10^{-14} \text{ J-s/m}^3;$$

hence

$$\frac{B_{ul}}{A_{ul}} = 1.52 \times 10^{13} \text{ m}^3/\text{J-s}.$$

We must now compute the energy density $u(\nu)$, which from (6.35) is related to the intensity per unit frequency $I(\nu)$ as $u(\nu) = I(\nu)/c$. We can compute $I(\nu)$ by dividing the laser beam power in the cavity by the beam cross-sectional area and the frequency width of the beam. The power of the beam within the cavity traveling toward the output mirror must be 100 mW and that reflected would be 99 mW (1 mW passes through the mirror). Thus, the total power in the cavity is 199 mW. The Doppler width of the helium–neon 632.8-nm transition (see Table 4-1) is 1.5×10^9 Hz. Thus

$$u(\nu) = \frac{I(\nu)}{c}$$
$$= \frac{[(199 \times 1.0 \text{ mW})/(\pi \cdot (5 \times 10^{-4} \text{ m})^2)]/(0.1)(1.5 \times 10^9 \text{ Hz})}{3 \times 10^8 \text{ m/s}}$$
$$= 5.63 \times 10^{-12} \text{ J-s/m}^3,$$

so the ratio is

$$\frac{B_{ul}u(\nu)}{A_{ul}} = (1.52 \times 10^{13} \text{ m}^3/\text{J-s})(5.63 \times 10^{-12} \text{ J-s/m}^3) = 85.6.$$

The stimulated emission rate is therefore almost 86 times the spontaneous emission rate on transitions from the upper to the lower laser level at 632.8 nm.

Using (6.57), the preceding ratio can be rewritten as

$$\frac{B_{ul}u(\nu)}{A_{ul}} = \frac{1}{e^{h\nu_{ul}/kT} - 1} = 85.6,$$

which yields

$$e^{h\nu_{ul}/kT} - 1 = 1/85.6 = 0.0117$$

or

$$h\nu_{ul}/kT = \ln(1.0117) = 1.16 \times 10^{-2}.$$

We can thus solve for T as follows:

$$T = \frac{h\nu_{ul}}{(1.16 \times 10^{-2})k} = \frac{(6.63 \times 10^{-34}\ \text{J-s})(4.74 \times 10^{14}\ \text{Hz})}{(1.16 \times 10^{-2})(1.38 \times 10^{-23}\ \text{J/K})}$$
$$= 1.96 \times 10^{6}\ \text{K} = 1{,}960{,}000\ \text{K}.$$

This calculation indicates that the radiation intensity of the laser beam inside the laser cavity has a value equivalent to that of a nearly 2,000,000-K blackbody – if we consider only the radiation emitted from the blackbody in the frequency (or wavelength interval) over which the laser operates.

REFERENCES

A. Corney (1977), *Atomic and Laser Spectroscopy.* Oxford: Clarendon Press, Chapter 9.
R. B. Leighton (1959), *Principles of Modern Physics.* New York: McGraw-Hill, Chapter 2.
R. Loudon (1973), *The Quantum Theory of Light.* Oxford: Clarendon Press, Chapter 1.

PROBLEMS

1. Calculate the number of radiation modes in a cube 1 mm on a side for a spread of 0.001 nm centered at 514.5 nm and a spread of 0.01 μm centered at 10.6 μm.
2. Consider a 1-mm–diameter surface area of carbon (graphite). Calculate how many atoms would exist in energy levels from which they could emit radiation at wavelengths shorter than 700 nm (visible light and shorter wavelengths) for surface temperatures of 300 K, 1,000 K, and 5,000 K when the solid is in thermal equilibrium at those temperatures. Assume that only those atoms within a depth of 10 nm of the material surface can emit observable radiation.
3. In Problem 2, if the excited atoms that emit visible radiation decay in 10^{-13} s and if only 0.002% of them decay radiatively (quantum yield of 2%), how much power would be radiated from that surface at the aforementioned temperatures? Assume that half of the atoms that radiate emit into the 2π solid angle that would result in their leaving the surface of the material, and assume an average visible photon energy of 2.5 eV. Also compute the total amount of power that could be radiated (over all wavelengths) from the surface at the given temperatures using the Stefan–Boltzmann law (eqn. 6.15). Speculate as to why the two approaches for computing the radiated power are inconsistent at a temperature of 5,000 K.
4. How much power is radiated from a 1-mm^2 surface of a body at temperature T when the peak measured wavelength is that of green light at 500 nm?
5. Determine the number of modes in a 1-cm^3 box for frequencies in the visible spectrum between 400 and 700 nm. Compare that value to the number of modes in a

sodium streetlamp that emits over a wavelength interval of 3 nm at a center wavelength of 589 nm. Assume that the streetlamp is a cylinder of radius 0.5 cm and length 10 cm.

6. Estimate the number of photons in both the box and the streetlamp of Problem 5 for temperatures of 300 K, 1,000 K, and 5,000 K.

7. A 100-W incandescent lamp has a tungsten filament composed of a wire, 0.05 cm in diameter and 10 cm in length, that is coiled up to fit within the light bulb. Assume the filament is heated to a temperature of 3,000 K when the light bulb is turned on. How much power (watts) is emitted within the visible spectrum from the filament, assuming that it is emitting as a blackbody? As an approximation, you could divide the visible spectral region into several segments and compute the average contribution from each segment. Then simply add the averages together (instead of trying to integrate the blackbody function over the entire visible spectral range).

8. Show that Planck's radiation law of (6.39) will lead to the Stefan–Boltzmann relationship of (6.15) if the power radiated over all wavelengths is considered. Determine the coefficients of the Stefan–Boltzmann constant. *Hint:*

$$\int_0^\infty \frac{x^3\,dx}{e^x - 1} = \frac{\pi^4}{15}.$$

9. An argon ion laser emits 2 W of power at 488.0 nm in a 2-mm–diameter beam. What would be the effective blackbody temperature of the output beam of that laser radiating over the frequency width of the laser transition, given that the laser linewidth is approximately one fifth of the Doppler linewidth? Assume that the laser is operating at an argon gas temperature of 1,500 K and that the laser output is uniform over the width of the beam.

10. For the laser in Problem 9, how much power would be required for the stimulated emission rate to equal the radiative decay rate?

11. A pulsed and Q-switched Nd:YAG laser is focused to a 200-μm–diameter spot size on a solid flat metal target in an attempt to produce a bright plasma source for microlithography applications. The plasma is observed to radiate uniformly into 2π steradians with a wavelength distribution that is approximately that of a blackbody. The intensity of the Nd:YAG laser is adjusted so that the peak of the blackbody emission occurs at a wavelength of 13.5 nm, the optimum wavelength as a source for EUV microlithography. What is the temperature of the blackbody? What fraction of the total energy radiated by the blackbody would be radiated within the useful bandwidth for microlithography of 0.4 nm centered around the emission maximum? Assume that the plasma doesn't expand significantly during the 10-ns emission time (the duration of the Nd:YAG laser pulses).

12. The blackbody spectral distribution curve has a maximum wavelength λ_m that is dependent upon the temperature T of the radiating body. Show that the product $\lambda_m T$ is a constant for any temperature (Wien's law, eqn. 6.16). *Hint:* Use the frequency version of the blackbody radiation formula instead of the wavelength version to show this.

13. A blue argon laser beam at 488 nm is propagating around a coliseum as part of a laser light show. The power is measured to be 10 W cw at a specific location with a beam diameter of 5 mm. What is the energy density per unit frequency $u(\nu)$ of the beam at that location?

are self-selected by the beam. The use of a short laser pulse allows heat to destroy the bad cells without the heat spreading to the surrounding cells. In the case of tattoo removal, the tattoo itself is absorbing and hence requires no tagging. Other applications include pollution detection and removal of kidney stones.

TITANIUM SAPPHIRE LASER

General Description

The titanium sapphire laser ($Ti:Al_2O_3$) is the most widely used tunable solid-state laser. It can be operated over a wavelength range of 660–1,180 nm and thus has the broadest gain bandwidth of any laser. It also has a relatively large stimulated emission cross section for a tunable laser. Titanium ions are typically doped into a sapphire (aluminum oxide) crystal at a concentration of 0.1% by weight. This laser has achieved cw outputs of nearly 50 W as well as terawatts of peak power from 100-fs–duration mode-locked pulses. The laser can be flashlamp pumped, but the technique is not efficient owing to the unusually short upper laser level lifetime of the laser crystal (3.8 μs at room temperature), which does not match well with the longer pulse duration of typical flashlamps. Commercial titanium sapphire lasers are therefore typically pumped with either argon ion lasers (for cw operation) or frequency-doubled Nd:YAG or Nd:YLF lasers (for pulsed operation). The pump absorption band covers the range from less than 400 nm to just beyond 630 nm and peaks around 490 nm, as can be seen in Figure 15-13. The titanium sapphire crystal has high thermal conductivity, good chemical inertness, good mechanical rigidity, and high hardness.

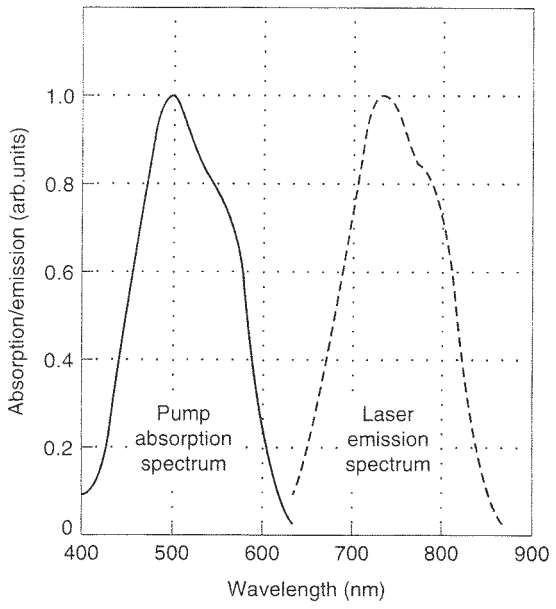

Figure 15-13 Absorption and emission spectra of titanium:sapphire laser amplifier rod

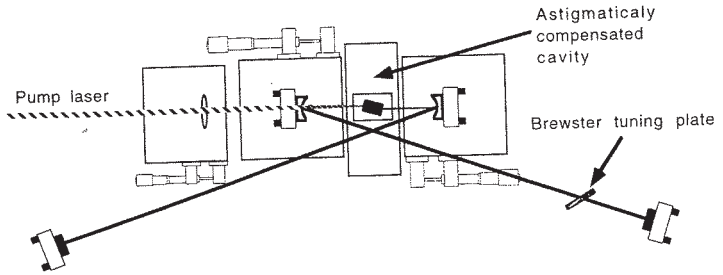

(a) cw Ti:sapphire - X fold configuration

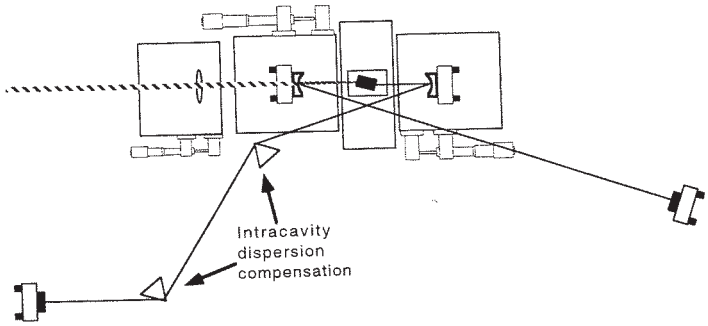

(b) Femtosecond mode-locked Ti:sapphire

Figure 15-14 Diagrams of (a) a cw titanium sapphire laser and (b) a femtosecond mode-locked titanium sapphire laser (courtesy of CREOL)

Laser Structure

An example of a cw Ti:Al_2O_3 laser using an X-cavity design is shown in Figure 15-14(a). It uses an astigmatically compensated cavity for the Ti:Al_2O_3 laser crystal (see Section 13.9). In such a cavity design, the crystal typically ranges from 2 to 10 mm in length, depending upon the dopant level, and is arranged with the output faces of the crystal at Brewster's angle. The longer-length crystal lengths with lower doping concentrations are used with higher pumping flux intensities in order to obtain higher power output. Generally, either a cw argon ion laser or a doubled Nd:YAG laser is used as the pumping source. The pump beam enters the cavity from the left, as shown in the figure. A birefringent filter, installed within the cavity at Brewster's angle, can be rotated for wavelength tuning. A modified version of this cavity, shown in Figure 15-14(b), is used to produce mode-locked pulses. It includes two prisms for intracavity dispersion compensation and uses the Kerr lens mode-locking (KLM) technique described in Section 13.4. The necessary aperture within the Ti:Al_2O_3 crystal to produce KLM is provided by a separate aperture located next to the crystal (not shown), or simply by the aperturing effect associated with the small diameter of the pump beam. Extremely precise adjustments and alignment of the mirrors and cavity dimensions are essential to maintain a stable mode-locked output for this laser.

Excitation Mechanism

The energy-level structure of this laser is similar to that of a dye laser. The ground state, a $^2T_2$ state, has a broad sequence of overlapping vibrational or vibronic levels extending upward from the lowest level, as shown in Figure 5-16. The first excited state is a ^2E state that also extends upward with a series of overlapping vibronic levels. This energy-level structure is unique for laser crystals in that there are no d-state energy levels above the upper laser level. Thus, the simple energy-level structure involving a 3d electron eliminates the possibility of excited-state absorption, an effect that reduces the tuning range of other tunable solid-state lasers (see Section 9.5).

Excitation therefore occurs from the lowest vibronic levels of the $^2T_2$ ground state (those that are sufficiently populated at room temperature) to the broad range of excited vibronic levels of the ^2E excited state. The population pumped to all of the vibrational levels of the broadband excited state rapidly relaxes to the lowest levels of that state. It then decays back to any one of the vibronic levels of the ground state in a manner that is similar to a dye laser, but with a much lower radiative rate. When the population reaches the excited vibronic levels of the ground state, it very rapidly relaxes to the lowest-lying levels, leaving a distribution dictated by the Boltzmann relationship of (6.11).

TABLE 15-11

Typical Titanium Sapphire Laser Parameters

Laser wavelengths (λ_{ul})	660–1,180 nm
Laser transition probability (A_{ul})	2.6×10^5/s
Upper laser level lifetime (τ_u)	3.8 μs
Stimulated emission cross section (σ_{ul})	3.4×10^{-23} m^2
Spontaneous emission linewidth and gain bandwidth, FWHM ($\Delta\nu_{ul}$)	1.0×10^{14}/s ($\Delta\lambda_{ul} = 180$ nm)
Inversion density (ΔN_{ul})	6×10^{23}/m^3
Small-signal gain coefficient (g_0)	20/m
Laser gain-medium length (L)	0.1 m
Single-pass gain ($e^{\sigma_{ul}\Delta N_{ul}L}$)	7–10
Doping density	3.3×10^{25}/m^3
Index of refraction of gain medium	1.76
Operating temperature	300 K
Thermal conductivity of laser rod	3.55 W/m-K
Thermal expansion coefficient of laser rod	5×10^{-6}/K
Pumping method	optical (flashlamp or laser)
Pumping bands	380–620 nm
Output power	up to 50 W (cw), 10^{12} W for 100-fs pulse
Mode	single-mode or multi-mode

The laser energy-level arrangement is effectively a four-level system, as in a dye laser, in which all of the higher-lying vibronic levels of the ^{2}E state serve as level i of the four-level system described in Section 9.3. The lowest vibrational levels of the ^{2}E state serve as the upper laser level u. These levels decay to any of the excited vibrational levels of the ground state $^2T_2$, any of which can be considered as the lower laser level l. These levels then rapidly relax to the lowest levels of $^2T_2$ serving as the ground state 0.

Applications

Titanium sapphire lasers are used in infrared spectroscopy of semiconductors and in laser radar, rangefinders, and remote sensing. They are used in medical applications such as photodynamic therapy. They are also used to produce short pulses of X-rays by focusing the mode-locked pulses onto solid targets from which high-density and high-temperature radiating plasmas are produced, plasmas that in turn emit large fluxes of X-rays.

CHROMIUM LiSAF AND LiCAF LASERS

General Description

The chromium-doped lithium strontium aluminum fluoride (Cr:LiSAF) and lithium calcium aluminum fluoride (Cr:LiCAF) lasers are broadband tunable lasers in the same category as the alexandrite and titanium sapphire lasers. The Cr:LiSAF laser can be tuned over a wavelength ranging from 780 to 1,010 nm and the Cr:LiCAF laser can be tuned from 720 to 840 nm. Both cw and pulsed output have been obtained from both lasers: a cw output of up to 1.2 W and a pulsed output of over 10 J with a slope efficiency of 5%. These lasers have relatively long upper-level lifetimes of 67 μs for Cr:LiSAF and 170 μs for Cr:LiCAF, so both can be effectively flashlamp pumped. They have also been laser pumped with AlGaAs diode lasers and argon ion lasers. Both of these fluoride laser materials can be doped to very high concentrations (up to 15% Cr) without affecting the upper laser level lifetime, which results in more uniform flashlamp pumping as indicated in Figure 10-19(c). These lasers have also been used as regenerative amplifiers leading to very short–pulse amplification. The laser crystals are chemically stable when treated properly. Their thermal properties are closer to those of Nd:glass than to Nd:YAG. They are durable but not as hard as YAG. Their average power-handling capabilities are not as good as Ti:Al_2O_3.

Laser Structure

A diagram of a flashlamp-pumped Cr:LiSAF laser is shown in Figure 15-15. This laser uses a LiSAF rod of 6-mm diameter and 0.1-m length. A birefringent filter is used to tune the wavelength from 750 to 1,000 nm, and a saturable absorber is